Journal of Visualized Experiments
Experimental and data analysis workflow for soft matter nanoindentation
--Manuscript Draft--

Article Type:	Invited Methods Collection - JoVE Produced Video
Manuscript Number:	JoVE63401R2
Full Title:	Experimental and data analysis workflow for soft matter nanoindentation
Corresponding Author:	Giuseppe Ciccone University of Glasgow Glasgow, UNITED KINGDOM
Corresponding Author's Institution:	University of Glasgow
Corresponding Author E-Mail:	g.ciccone.1@research.gla.ac.uk
Order of Authors:	Giuseppe Ciccone
	Mariana Azevedo Gonzalez Oliva
	Nelda Antonovaite
	Ines Lüchtefeld
	Manuel Salmeron-Sanchez
	Massimo Vassalli

Additional Information:	
Question	**Response**
Please specify the section of the submitted manuscript.	Bioengineering
Please indicate whether this article will be Standard Access or Open Access.	Standard Access ($1400)
Please indicate the **city, state/province, and country** where this article will be **filmed**. Please do not use abbreviations.	Glasgow, UK
Please confirm that you have read and agree to the terms and conditions of the author license agreement that applies below:	I agree to the UK Author License Agreement (for UK authors only)
Please confirm that you have read and agree to the terms and conditions of the video release that applies below:	I agree to the Video Release
Please provide any comments to the journal here.	

1 **TITLE:**
2 Experimental and Data Analysis Workflow for Soft Matter Nanoindentation
3
4 **AUTHORS AND AFFILIATIONS:**
5 Giuseppe Ciccone[1], Mariana Azevedo Gonzalez Oliva[1], Nelda Antonovaite[2], Ines Lüchtefeld[3],
6 Manuel Salmeron-Sanchez[1], Massimo Vassalli[1]
7
8 [1]Centre for the Cellular Microenvironment, James Watt School of Engineering, University of
9 Glasgow, Glasgow, UK
10 [2]Optics 11 life, De Boelelaan 1081, 1081 HV Amsterdam, The Netherlands
11 [3]Laboratory of Biosensors and Bioelectronics, ETH Zürich, Gloriastrasse, Zürich, Switzerland
12
13 Email addresses of co-authors:
14 Giuseppe Ciccone   (g.ciccone.1@research.gla.ac.uk)
15 Mariana Azevedo Gonzalez Oliva   (m.azevedo-gonzalez-oliva.1@research.gla.ac.uk)
16 Nelda Antonovaite   (nelda@optics11.com)
17 Ines Lüchtefeld   (luechtefeld@biomed.ee.ethz.ch)
18 Manuel Salmeron-Sanchez   (manuel.salmeron-sanchez@glasgow.ac.uk)
19 Massimo Vassalli   (massimo.vassalli@glasgow.ac.uk)
20
21 Corresponding authors:
22 Giuseppe Ciccone   (g.ciccone.1@research.gla.ac.uk)
23 Mariana Azevedo Gonzalez Oliva   (m.azevedo-gonzalez-oliva.1@research.gla.ac.uk)
24

25 **KEYWORDS:**
26 nanoindentation, mechanical properties, mechanobiology, cell mechanics, elasticity,
27 hydrogels, soft matter, data analysis
28

29 **SUMMARY:**
30 The protocol presents a complete workflow for soft material nanoindentation experiments,
31 including hydrogels and cells. First, the experimental steps to acquire force spectroscopy data
32 are detailed; then, the analysis of such data is detailed through a newly developed open-
33 source Python software, which is free to download from GitHub.
34

35 **ABSTRACT:**
36 Nanoindentation refers to a class of experimental techniques where a micrometric force
37 probe is used to quantify the local mechanical properties of soft biomaterials and cells. This
38 approach has gained a central role in the fields of mechanobiology, biomaterials design, and
39 tissue engineering, to obtain a proper mechanical characterization of soft materials with a
40 resolution comparable to the size of single cells (μm). The most popular strategy to acquire
41 such experimental data is to employ an atomic force microscope (AFM); while this instrument
42 offers an unprecedented resolution in force (down to pN) and space (sub-nm), its usability is
43 often limited by its complexity that prevents routine measurements of integral indicators of
44 mechanical properties, such as Young's Modulus (E). A new generation of nanoindenters, such
45 as those based on optical fiber sensing technology, has recently gained popularity for its ease
46 of integration while allowing to apply sub-nN forces with μm spatial resolution, therefore
47 being suitable to probe local mechanical properties of hydrogels and cells.

48

49 In this protocol, a step-by-step guide detailing the experimental procedure to acquire
50 nanoindentation data on hydrogels and cells using a commercially available ferrule-top
51 optical fiber sensing nanoindenter is presented. Whereas some steps are specific to the
52 instrument used herein, the proposed protocol can be taken as a guide for other
53 nanoindentation devices, granted some steps are adapted according to the manufacturer's
54 guidelines. Further, a new open-source Python software equipped with a user-friendly
55 graphical user interface for the analysis of nanoindentation data is presented, which allows
56 for screening of incorrectly acquired curves, data filtering, computation of the contact point
57 through different numerical procedures, the conventional computation of E, as well as a more
58 advanced analysis particularly suited for single-cell nanoindentation data.

59

60 **INTRODUCTION:**

61 The fundamental role of mechanics in biology is nowadays established[1,2]. From whole tissues
62 to single cells, mechanical properties can inform about the pathophysiological state of the
63 biomaterial under investigation[3,4]. For example, breast tissue affected by cancer is stiffer than
64 healthy tissue, a concept that is the basis of the popular palpation test[5]. Notably, it has been
65 recently shown that the coronavirus disease 2019 (COVID-19) caused by severe acute
66 respiratory syndrome coronavirus 2 (SARS-CoV-2) is underlined by changes in the mechanical
67 properties of blood cells, including decreased erythrocyte deformability and decreased
68 lymphocyte and neutrophil stiffness as compared to blood cells from SARS-CoV-2-naïve
69 individuals[6].

70

71 In general, the mechanics of cells and tissues are inherently intertwined: each tissue has
72 specific mechanical properties that simultaneously influence and depend on those of the
73 constituent cells and extracellular matrix (ECM)[5]. Because of this, strategies to study
74 mechanics in biology often involve engineering substrates with physiologically relevant
75 mechanical stimuli to elucidate cell behavior in response to those stimuli. For example, the
76 seminal work by Engler and colleagues demonstrated that mesenchymal stem cell linage
77 commitment is controlled by matrix elasticity, as studied on soft and stiff two-dimensional
78 polyacrylamide (PAAm) hydrogels[7].

79

80 Many strategies to mechanically characterize the biomaterial under investigation exist,
81 varying in spatial scale (i.e., local to bulk) and in the mode of deformation (e.g., axial vs shear),
82 consequently yielding different information, which needs careful interpretation[3,8–10]. The
83 mechanics of soft biomaterials is commonly expressed in terms of stiffness. However,
84 stiffness depends on both material properties and geometry, whereas elastic moduli are
85 fundamental properties of a material and are independent of the material's geometry[11]. As
86 such, different elastic moduli are related to the stiffness of a given sample, and each elastic
87 modulus encompasses the material's resistance to a specific mode of deformation (e.g., axial
88 vs shear) under different boundary conditions (e.g., free expansion vs confinement)[11,12].
89 Nanoindentation experiments allow the quantification of mechanical properties through
90 Young's modulus (E), which is associated with uniaxial deformation (indentation) when the
91 biomaterial is not laterally confined[10–12].

92

93 The most popular method to quantify the E of biological systems at the microscale is atomic
94 force microscopy (AFM)[13–16]. AFM is an extremely powerful tool with force resolution down

95 to the pN level and spatial resolution down to the sub-nm scale. Further, AFM offers extreme
96 flexibility in terms of coupling with complementary optical and mechanical tools, extending
97 its capabilities to extract a wealth of information from the biomaterial under investigation[13].
98 Those attractive features, however, come with a barrier-to-entry represented by the
99 complexity of the experimental set-up. AFM requires extensive training before users can
100 acquire robust data, and its use for everyday mechanical characterization of biological
101 materials is often unjustified, especially when its unique force and spatial resolutions are not
102 required.
103
104 Because of this, a new class of nanoindenters has recently gained popularity due to their ease
105 of use, while still offering AFM-comparable data with sub nN force resolution and μm spatial
106 resolution, reflecting forces exerted and perceived by cells over relevant length scales[2].
107 Particularly, ferrule-top nanoindentation devices based on optical fiber sensing
108 technology[17,18] have gained popularity among researchers active in the field of
109 mechanobiology and beyond; and a wealth of works reporting the mechanical properties of
110 biomaterials using those devices, including cells[19,20], hydrogels[8,21], and tissues[22,23] have been
111 published. Despite the capabilities of those systems to probe local dynamic mechanical
112 properties (i.e., storage and loss modulus), quasi-static experiments yielding E remain the
113 most popular choice[8,19–21]. In brief, the system consists of indenting the sample with a
114 constant speed up to a set-point defined either by a maximum displacement, force, or
115 indentation depth, and recording both the force and the vertical position of the cantilever in
116 so-called force-distance (F-z) curves. F-z curves are then converted into force-indentation (F-
117 δ) curves through the identification of the contact point (CP), and fitted with an appropriate
118 contact mechanics model (usually the Hertz model[13]) to compute $E.$
119
120 While the operation of ferrule-top nanoindenters resembles AFM measurements, there are
121 specificities worth considering. In this work, a step-by-step guide to robustly acquire F-z
122 curves from cells and tissue-mimicking hydrogels using a commercially available ferrule-top
123 nanoindenter is provided, in order to encourage standardization of experimental procedures
124 between research groups using this and other similar devices. In addition, advice on how to
125 best prepare hydrogel samples and cells to perform nanoindentation experiments is given,
126 together with troubleshooting tips along the experimental pathway.
127
128 Furthermore, much of the variability in nanoindentation results (i.e., E and its distribution)
129 depends on the specific procedure used to analyze data, which is non-trivial. To address this
130 issue, instructions for the use of a newly developed open-source software programmed in
131 Python and equipped with a user-friendly graphical user interface (GUI) for batch analysis of
132 F-z curves are provided. The software allows for fast data screening, filtering of data,
133 computation of the CP through different numerical procedures, the conventional
134 computation of E, as well a more advanced analysis named the elasticity spectra[24], allowing
135 to estimate the cell's bulk modulus (E_b), actin cortex's modulus (E_0), and actin cortex's
136 thickness (d_0). The software can be freely downloaded from GitHub and can be easily adapted
137 to analyze data originating from other systems by adding an appropriate data parser. It is
138 emphasized that this protocol can be used for other ferrule-top nanoindentation devices, and
139 other nanoindentation devices in general, granted some steps are adapted according to the
140 specific instrument's guidelines. The protocol is schematically summarized in **Figure 1**.
141

PROTOCOL:

1.   Preparation of substrates/cells for nanoindentation measurements

1.1   Follow the steps given in the **Supplementary Protocol** for preparation of PAAm hydrogels/cells for nanoindentation experiments. The procedure is summarized in **Figure 2**.

NOTE: PAAm hydrogels have been chosen as they are the most common hydrogels used within the field of mechanobiology. However, the protocol is equally applicable to any type of hydrogel[25] (see **Discussion**, modifications of the method).

2.   Starting up the device, probe choice, and probe calibration

2.1   Follow the steps given in the **Supplementary Protocol** for starting up the device. For technical details on the operation of optical fiber, ferrule-top nanoindenters check these references[17,18].

2.2   Select the nanoindentation probe as described below.

NOTE: All commercially available probes such as the ones used in this protocol are equipped with a spherical tip (**Figure 3A**). Therefore, the choice narrows down to two variables: the cantilever's stiffness and tip radius (**Figure 3B**).

2.2.1   Choose a cantilever's stiffness (k in N/m) that matches the expected sample stiffness for best results[15] (see **Figure 3C** and **Discussion**, critical steps in the protocol). For cells, select a probe with k in the range 0.01–0.09 N/m. For hydrogels, select a probe with k in the range 0.1–0.9 N/m, which yields optimal results for gels with expected E between a few kPa and 100 kPa (see **Representative Results**).

2.2.2   Choose the tip radius (R in μm) according to the desired spatial resolution of the indentation process. For small cells such as HEK293 cells (average diameter of ~10–15 μm[26]) select a sphere with R = 3 μm. For hydrogels, select a sphere with R = 10–250 μm to probe the biomaterial's mechanical properties over a large contact area and avoid local heterogeneities.

2.2.3   Consult **Figure 3C** and any additional manufacturer's guidelines to select the appropriate probe.

2.3   Once the probe has been selected, follow the steps in the **Supplementary Protocol** to mount it on the nanoindenter.

3.   Probe calibration

NOTE: The following steps are specific to ferrule-top nanoindentation devices based on optical fiber sensing technology, and they are detailed for software version 3.4.1. For other nanoindentation devices, follow the steps recommended by the device manufacturer.

189 3.1   On the software's main window, click on **Initialize**. A calibration menu will appear.
190 Enter the probe details (can be found on the side of the probe's box; k in N/m, R in μm, and
191 the calibration factor in air) in the input boxes.
192
193 3.2   Prepare the calibration dish: a thick glass Petri dish with a flat bottom (see **Discussion,**
194 critical steps in the protocol). Fill the dish with the same medium as the sample dish (this can
195 also be air). Match the temperature of the medium with that of the sample.
196
197 3.3   Place the calibration dish under the probe. If required, slide out the probe from the
198 nanoindenter's arm holder and hold it in one hand to make space for placement of the
199 calibration dish. Slide back the probe into place.
200
201 3.4   Perform the next two steps for calibration in liquid. If measuring in the air, use the
202 provided polytetrafluoroethylene substrate for calibration and skip to step 3.5.
203
204 3.4.1   Prewet the probe with a drop of 70% ethanol using a Pasteur pipette with the end of
205 the pipette in light contact with the glass ferrule, for the drop to slide over the cantilever and
206 spherical tip[27] (see **Discussion**, critical steps in the protocol).
207
208 3.4.2   Manually slide the nanoindenter's arm downwards until the probe is fully submerged,
209 but still far away from the bottom of the Petri dish. If required, add more medium to the
210 calibration dish. Wait 5 min so that equilibrium conditions are reached in the liquid.
211
212 3.5   In the software's **Initialize** menu, click on **Scan Wavelength.** The interferometer's
213 screen will show a progress bar. To check whether the optical scan was successful, navigate
214 to the **Wavelength Scan** panel on the interferometer box. If successful, a sine wave should be
215 visible (**Figure S1A**). See **Discussion** (troubleshooting of the method) if an error appears.
216
217 3.6   In the **Initialize** menu, click on **Find Surface**, which will progressively lower the probe
218 until a set threshold in the cantilever's bending is reached. The probe stops moving when
219 contact with the glass Petri dish is made.
220
221 3.7   Check whether the probe is in contact with the surface. Move the probe down by 1
222 μm using the y downwards arrow button on the software's main window. Observe the green
223 signal in the **Live Window** of the software for changes in the baseline with each step, when
224 the cantilever is in contact with the substrate (**Figure S1B**). If there is no change, the cantilever
225 is not in contact (see next step).
226
227 3.8   Increase the **Threshold** value in the **Options** menu under the **Find Surface** tab from its
228 default value of 0.01 by a step of 0.01 at a time and repeat the **Find Surface** step until in
229 contact. Alternatively, bring down the probe to contact in small 1 μm steps until the green
230 baseline starts shifting at each downwards step.
231
232 NOTE: For the softest cantilevers ($k = 0.025$ Nm^{-1}), increase the **Threshold** value in the **Options**
233 menu under the **Find Surface** tab a priori of performing step 3.6. Start from a threshold value
234 of 0.06 or 0.07 and increase it up to 0.1 if necessary. This is because environmental noise will

235 likely cause the cantilever to bend above the threshold prior to contact. For soft probes,
236 decreasing the **Approach Speed (μm/s)** in the same menu also improves the procedure.
237
238 3.9   In the **Initialize** menu, click on **Calibrate**.
239
240 3.10   Check the **Live Signal** window of the software and make sure that both piezo and
241 cantilever signals move up at the same time (**Figure S1C**).
242
243 3.10.1 If there is a mismatch in time, the probe is not fully in contact with the glass. Move
244 down the probe at steps of 1 μm until the baseline of the cantilever signal changes (see step
245 3.7) and repeat step 3.9.
246
247 3.10.2 If the cantilever signal does not change at all during the **Calibrate** step, then the probe
248 is far from the surface. Increase the contact threshold iteratively (see step 3.8) until the
249 surface is found correctly and repeat calibration from the beginning starting with the
250 wavelength scan.
251
252 3.11   When the calibration is complete, check the old and new calibration factors on the
253 pop-up window displayed. If the new calibration factor is in the correct range, click on **Use**
254 **New Factor**. If calibration fails, and the new factor is either NaN or is not in the expected
255 range, see **Discussion** (troubleshooting of the method) for resolution.
256
257 NOTE: The new factor should be ˜n times lower than the one provided on the probe's box if
258 the calibration was performed in a liquid medium with refractive index n (n = 1.33 for water).
259 If calibration was performed in air, then the new and old calibration factors should be
260 approximately equal.
261
262 3.12   Move up the piezo by 500 μm.
263
264 3.13   Check whether the demodulation circle has been correctly calibrated as follows.
265 Navigate to the **Demodulation** tab on the interferometer desktop. Gently tap on the optical
266 table or on the nanoindenter to induce enough noise. A white circle made up of discrete data
267 points should approximately cover the red circle (**Figure S1D**).
268
269 3.14   If the white circle does not overlap with the red circle, or a warning appears on the
270 interferometer's display, the demodulation circle needs recalibration. This can be done in two
271 ways as described below.
272
273 3.14.1 Continuously tap on the body of the nanoindenter to induce one full circle of noise
274 and press the **Calibrate** button on the interferometer.
275
276 3.14.2 Enter in contact with the glass substrate and press **Calibrate** from the **Initialize** menu
277 of the software's main window. Do not save the calibration factor. At this point, check again
278 and make sure the white circle overlaps with the red circle.
279
280 NOTE: If the signal is not just slightly displaced from the demodulation circle but rather
281 became very small or is not visible at all, it means that the cantilever is stuck to the optical

282   fiber. Follow the troubleshooting advice for this problem (see **Discussion,** troubleshooting of
283   the method) and repeat either steps 3.14.1 or 3.14.2. Once the cantilever gets back to its
284   horizontal position (**Figure 3A**), the signal will recover to the demodulation circle.

286   3.15   Verify the calibration by performing an indentation on the glass substrate directly
287   after the calibration as described below.

289   3.15.1 Load or make an experiment file by clicking on **Configure Experiment** and add a find
290   surface step and indentation step. For the indentation step, use the default displacement
291   mode settings and change the maximum displacement to the calibration distance (3,000 nm)
292   to displace the probe again on the stiff substrate.

294   3.15.2 Click on **Run Experiment** and check the demodulation circle in the interferometer
295   window. Check the white signal and make sure it is on top of the red circle during indentation.

297   3.15.3 Check the results on the software's main window in the **Time Data** graph, and make
298   sure the piezo displacement (blue line) is equal to the cantilever bending (green line) as the
299   indentation starts in contact and no material deformation is expected. If the signals are not
300   parallel, see **Discussion** (troubleshooting of the method).

302   3.16   Change the local path in the calibration menu by setting the **Calibration Save Path** to
303   an appropriate directory.

305   3.17   When the probe has been successfully calibrated, move the piezo up by 500 μm.

307   **4.   Measuring the Young's Modulus of soft materials**

309   4.1   Nanoindentation of hydrogels

311   4.1.1   Load the Petri dish containing the sample(s) on the microscope's stage and manually
312   move the nanoindenter's probe to a desired *x-y* position above the sample.

314   4.1.2   Manually slide the probe in solution, taking care to leave 1–2 mm between the probe
315   and the sample's surface at this stage. Wait 5 min for the probe to equilibrate in the medium.

317   4.1.3   Focus the *z* plane of the optical microscope so that the probe is clearly visible.

319   4.1.4   Perform a single indentation to tune the experimental parameters as described below.

321   4.1.4.1 Configure a new experiment in the software's main window. Click on **Configure**
322   **Experiment**, which will open a new window. Add a **Find Surface** step. All parameters of the
323   **Find Surface** step can be changed in the **Options** menu of the software if required.

325   NOTE: The **Find Surface** will lower the probe until the surface is found, and then it will retract
326   the probe to a distance defined by **Z Above Surface (μm),** above the sample's surface. If the
327   selected cantilever is too stiff for the sample or the sample is sticky, after the step the probe
328   is likely to still be in contact with the sample, which will result in a curve without a baseline

329   (**Figure 4C**). To solve this problem, increase the **Z Above Surface (μm)**.

331   4.1.4.2 Add an indentation step. Select the **Profile** tab and click on **Displacement Control**. For
332   single indentation, leave the default indentation profile.

334   4.1.4.3 Click on **Run Experiment** on the main software window. This will find the surface and
335   perform a single indentation. If the single indentation does not look as expected, adjust the
336   experimental parameters as outlined in **Figure 4** and **Discussion** (troubleshooting of the
337   method).

339   4.1.5   Once the indentation looks as desired, configure the matrix scan so that a sufficient
340   area of the sample will be indented. Click on **Configure Experiment**, add a **Find Surface** step
341   with the previously determined experimental parameters and add a **Matrix Scan** step.

343   4.1.6   For flat hydrogels, configure a matrix scan containing 50–100 points (i.e., 5 x 10 or 10
344   x 10 in *x* and *y*) spaced at 10–100 μm (i.e., *dx* = *dy* = 10-100 μm). Click on **Use Stage Position**
345   to start the matrix scan from the current stage position. Make sure the **Auto Find Surface** box
346   is ticked to find the surface at each indentation using the set experimental parameters.

348   4.1.6.1 To avoid oversampling, set the step size to at least twice the contact radius ($a = \sqrt{R\delta}$,
349   where δ is the indentation depth).

351   4.1.6.2 Set up the matrix scan profile in displacement control. Ensure that the profile does not
352   violate the assumptions of the Hertz model (see **Discussion**, critical steps in the protocol).

354   4.1.6.3 Leave the number of segments to 5, which is the default value, and use the default
355   displacement profile. If necessary, change the displacement profile in terms of maximum
356   displacement and time for each sloped segment, which will affect the maximum indentation
357   depth and the strain rate, respectively. Do not exceed strain rates > 10 μm/s (see **Discussion**,
358   limitations of the method).

360   4.1.6.4 Enter a value for the approach speed, which determines how fast the probe is
361   displaced toward the sample before contact. Match the retraction speed to the approach
362   speed (see note below).

364   NOTE: For soft cantilevers and noisy environments, an approach speed of 1,000–2,000 nm/s
365   is recommended. For stiffer cantilevers and controlled environments, this can be increased.

367   4.1.6.5 Save the configured experiment in the desired **Experiment Path** and select a directory
368   where the data will be saved in the **Save Path**, in the **General** tab of the **Configure Experiment**
369   window. Click on **Run Experiment**.

371   4.1.7   Once the matrix scan is completed, raise the probe by 200–500 μm and move the
372   probe to a different area of the sample sufficiently far away from the first area.

374   4.1.8   Repeat the experiment at least two times so that sufficient data is acquired on each
375   sample (i.e., at least two matrix scans per sample, containing 50–100 curves each).

376

377 4.2 Nanoindentation of cells

378

379 4.2.1 Load the sample on the microscope as described above.

380

381 4.2.2 For single-cell indentation, focus the *z* plane so that both cells and probe are visible at
382 20x or 40x magnification, depending on cell size or spreading.

383

384 4.2.3 Move the probe above the cell to be indented.

385

386 4.2.4 Configure a new experiment in the software's main window. Click on **Configure**
387 **Experiment**, which will open a new window. Add a **Find Surface** and **Indentation** step with
388 default parameters in displacement mode.

389

390 4.2.5 Click on **Run Experiment**, which will find the surface and perform a single indentation.
391 Check whether the indentation was successful. If the curve does not look as expected, adjust
392 the experimental parameters (see **Figure 4** and **Discussion**, troubleshooting of the method).

393

394 4.2.6 If the indentation was successful, add a matrix scan to the experiment. Follow the
395 steps given for hydrogels' nanoindentation experiments; configure the matrix scan so that
396 the step size allows for a small area of the cell to be indented; 25 points spaced at 0.5–5 µm
397 for HEK cells.

398

399 4.2.6.1 Depending on the cell size, adapt the matrix scan to ensure the tip does not indent
400 outside the cell limit, i.e., doing a different map geometry or probing fewer points.

401

402 4.2.7 Click on **Run Experiment** and wait for it to be completed.

403

404 4.2.8 Once the matrix scan is completed, raise the probe out of contact (50 µm in the *z*
405 plane).

406

407 4.2.9 Move the probe above a new cell and repeat the process (see **Discussion**, critical steps
408 in the protocol).

409

410 4.3 Cleaning the probe and switching off the instrument

411

412 4.3.1 Follow the steps given in the **Supplementary Protocol** to clean the probe and switch
413 off the nanoindentation device.

414

415 **5.** **Data analysis**

416

417 5.1 Downloading and installing the software

418

419 5.1.1 Follow the steps given in the **Supplementary Protocol** to download and install the
420 software for data analysis[28,29].

421

422 5.2 Screening *F-z* curves and production of cleaned data set in JSON format

423

424   5.2.1   Launch **prepare.py** from the command line on the lab computer as outlined in steps
425   5.2.2 to 5.2.3.

426

427   5.2.2   If using a Windows computer, hold the shift key while right-clicking on the
428   **NanoPrepare** folder and click on **Open PowerShell Window Here**. Type the **python
429   prepare.py** command and press the **Enter** key. A GUI will pop up on your screen (**Figure S2**).

430

431   5.2.3   If using a MacOS computer, right-click on the **NanoPrepare** folder and click on **New
432   Terminal at Folder**. Type the **python3 prepare.py** command and press the **Enter** key, which
433   will launch the GUI (**Figure S2**).

434

435   5.2.4   Select the **NEW** data format from the drop-down list. If data is not loaded correctly,
436   then relaunch the GUI and select **OLD**.

437

438   NOTE: The **NEW** format works for data obtained using ferrule-top optical fiber sensing
439   nanoindentation devices with software version 3.4.1. This format will also work for previous
440   software versions, at least those belonging to nanoindenters installed in 2019–2020.

441

442   5.2.5   Click on **Load Folder**. Select a folder containing the data to be analyzed—single matrix
443   scan or multiple matrix scans. The top graph (**Raw Curves**) will be populated with the
444   uploaded data set. To visualize a specific curve, click on it. This will highlight it in green and
445   show it on the bottom graph (**Current Curve**).

446

447   5.2.6   Clean the data set using the tabs present on the right part of the GUI as outlined
448   below.

449

450   5.2.6.1 Use the Segment button to select the correct segment to be analyzed, which is the
451   forward segment of *F-z* curves. The specific number depends on the number of segments
452   selected in the nanoindentation software when performing experiments.

453

454   5.2.6.2 Use the **Crop 50 nm** button to crop the curves by 50 nm at the extreme left (if L is
455   ticked), right (if R is ticked), or both sides (if both R and L are ticked). Click this button several
456   times to crop as much as is required. Use this to remove artifacts present at the start/end of
457   *F-z* curves.

458

459   5.2.6.3 Inspect the **Cantilever** tab for the spring constant, tip geometry, and tip radius. Inspect
460   the tab to ensure that the metadata has been read correctly.

461

462   5.2.6.4 Use the **Screening** tab to set a force threshold that will discard all the curves that did
463   not reach the given force. Discarded curves will be highlighted in red.

464

465   5.2.6.5 Use the Manual **Toggle** button to manually remove curves that have not been
466   correctly acquired. Remove any curves by clicking on the specific curve and selecting **OUT**,
467   which will highlight the curve in red.

468

469   5.2.7   Click on **Save JSON**. Enter an appropriate name for the cleaned data set, which is a

470 single JSON file. Send the JSON file to the computer where the NanoAnalysis software was
471 installed.
472
473 6.   **Formal data analysis**
474
475 6.1   Launch the **nano.py** file from the command line by navigating to the NanoAnalysis
476 folder, opening it, and launching a terminal in the automatically created nanoindentation
477 folder. Type the **python nano.py** or **python 3 nano.py** command (depending on the operating
478 system) and press the **Enter** key. A GUI will pop up on your screen (**Figure S3**).
479
480 6.2   On the top left of the GUI, click on **Load Experiment** and select the **JSON** file. This will
481 populate the file list and the **Raw Curves** graph showing the data set in terms of F-z curves.
482 Both F and z axes are shown relative to the CP coordinates, which are computed in the
483 background when loading the dataset (see the following note). In the **Stats** box, check the
484 values of the three parameters: $N_{activated}$, N_{failed}, and $N_{excluded}$.
485
486 NOTE: $N_{activated}$ represents the number of curves that will be analyzed in the subsequent
487 Hertz/ES analysis and appear in black in the **Raw Curves** graph. N_{failed} represents the number
488 of curves on which a reliable CP could not be found and appear in blue in the graph. Those
489 curves will automatically be discarded in the subsequent analysis. Upon opening the software,
490 some curves may be automatically moved to the failed set. This is because the CP is calculated
491 upon opening the software with the default threshold algorithm (see below). $N_{excluded}$
492 represents the curves that are manually selected to be excluded from the analysis and will
493 appear in red in the graph (see below).
494
495 6.3   Check whether the number of failed, excluded, and activated curves are reasonable.
496 Check the **Raw Curves** graph to visualize the curves.
497
498 6.4   To visualize a specific curve in more detail, click on it. This will highlight it in green and
499 show it on the **Current Curve** graph. Once a single curve has been selected, the R and k
500 parameters (which must be the same for all curves) will be populated in the **Stats** box of the
501 GUI.
502
503 6.5   Change the status of a given curve using the **Toggle** box. Click on the specific curve
504 you want to change the status of, and then click on either **Activated**, **Failed,** or **Excluded**. The
505 count in the **Stats** box is automatically updated.
506
507 NOTE: To change the view of the data set in the **Raw Curves** graph use the **View** box. Click on
508 **All** to show all curves (i.e., activated, failed, and excluded in the respective colors). Click on
509 **Failed** to show the activated and the failed curves and click on **Activated** to only show the
510 activated curves. To reset the status of all curves between activated and excluded, click on
511 **Activated** or **Excluded** in the **Reset** box.
512
513 6.6   Once the dataset has been further cleaned, follow the data analysis pipeline outlined
514 below.
515
516 6.6.1   Filter any noise present in the curves using the filters implemented in the GUI

517   (**Filtering Box**), namely, a custom filter called Prominency filter, the Savitzky Golay[30,31]
518   (SAVGOL) filter, and a smoothing filter based on computing the median of the data in a given
519   window (median filter). See **Discussion** (critical steps in the protocol) for details on filters.

521   6.6.2   Inspect the filtered curves in the **Current Curve** graph. The filtered curve is shown in
522   black whereas the non-filtered version of the curve is shown in green.

524   NOTE: It is advised to filter the data as little as possible to preserve features of the original
525   signal. Over filtering may smooth out any differences present in the data. Working with the
526   prominency filter activated is enough for the Hertz analysis of nanoindentation data. If the
527   data is particularly noisy, then a SAVGOL or median filters may be additionally applied.

529   6.6.3   Select an algorithm to find the CP. In the **Contact Point** box, choose one of a series of
530   numerical procedures that have been implemented in the software, namely, the Goodness of
531   Fit (GoF)[32], Ratio of Variances (RoV)[32], Second derivative[33], or threshold[33]. See **Discussion**,
532   critical steps in the protocol for details on the algorithms.

534   NOTE: The CP is the point at which the probe comes into contact with the material and needs
535   to be identified in order to convert F-z data into F-δ data (for soft materials, δ is finite and
536   needs to be calculated). The selected algorithm will be applied to all active curves of the data
537   set, and curves where the algorithm fails to locate the CP robustly will be moved to the failed
538   set.

540   6.6.4   Adjust the algorithm's parameters to suit your dataset so that the CP is located
541   correctly as detailed in the **Discussion**, critical steps in the protocol. To view where the CP has
542   been found on a single curve, select the curve by clicking on it and click on **Inspect**. Check the
543   pop-up window that appears to identify where the CP has been located.

545   6.6.5   Check whether the red line that appears, which is the parameter the algorithm
546   computed in the selected region of interest, has a maximum or minimum value that
547   corresponds to the location of the CP (e.g., for the GoF, the parameter is the R^2). Repeat this
548   process for all curves if needed.

550   NOTE: The axes of the pop-up are in absolute coordinates so that the location of the CP can
551   be shown. Conversely, the axes of the **Raw Curves** and **Current Curve** graph are shown
552   relative to the CP, i.e., the location of the CP is (0,0).

554   6.6.6   Click on **Hertz Analysis**. This will generate three graphs described below.

556   6.6.6.1 **Check** F-δ for each curve in the dataset together with the average Hertz fit (red dashed
557   line).Adjust the indentation in nm up to which the Hertz model is fitted in the **Results** box
558   under **Max Indentation (nm)**. Set it to a maximum of ˜10% of R for the Hertz model to be
559   valid (see **Discussion**, critical steps in the protocol).

561   6.6.6.2 Check the average F-δ curve with error band showing one standard deviation (SD)
562   together with the average Hertz fit (red dashed line). Visualize the average Hertz fit on the
563   **Raw Curves** graph for reference and the Hertz fit for each curve on the **Current Curve**.

564

565 6.6.6.3 Check the scatter plot of *E* originating from fitting the Hertz model to each individual
566 curve.

567

568 6.6.7   Click on either the file name, *F-z* curve, *F-δ* curve, or a point on the scatter plot to
569 highlight the curve in each plot. If a data point in the scatter plot appears to lie outside the
570 distribution of the data, click on it and inspect the curve to which it belongs. Verify that the
571 CP has been located correctly by clicking on the **Inspect** button. Exclude the curve from the
572 analysis if necessary.

573

574 6.6.8   Inspect the **Results** box for the computed mean *E* and its SD ($E_\gamma \pm \sigma$) and make sure
575 they are reasonable for the given experiment.

576

577 6.6.9   In the **Save** box, click on **Hertz**. In the pop-up window, enter file name and directory.
578 Once done, click on **Save**. A .tsv file will be created. Open the .tsv file in any additional
579 software of preference and use the values for statistical analysis and further plotting.

580

581 NOTE: The file contains the *E* obtained from each curve and the mean *E* and its SD.
582 Additionally, the file contains metadata associated with the analysis, including the number of
583 curves analyzed, *R*, *k,* and the maximum indentation used for the Hertz model. This step is
584 optional. Click on **Average F-Ind** to export the average force and the average indentation,
585 together with one SD in the force.

586

587 6.6.10 For cell nanoindentation data, click on **Elasticity Spectra Analysis** (see **Representative
588 Results** and **Discussion**). Inspect the two plots produced, namely, *E* as a function of the
589 indentation depth ($E(\delta)$) for each curve, and the average $E(\delta)$ fitted by a model, which
590 allows to estimate the cell's actin cortex Young's modulus, the cell's bulk Young's modulus,
591 and the actin cortex thickness. Check the average $E(\delta)$ in the top graph in red.

592

593 6.6.11 Make sure the **Interpolate** box is checked, which ensures the derivative needed to
594 perform the elasticity spectra analysis is computed on the interpolated signal (see
595 **Representative Results**).

596

597 6.6.12 Inspect the **Results** box, reporting the cortex modulus ($E_0 \pm \sigma$), the bulk modulus
598 ($E_b \pm \sigma$), and the cortex thickness ($d_0 \pm \sigma$).

599

600 NOTE: The average elasticity spectra may appear noisy at first, with prominent sinusoidal
601 oscillations. As a result, equation 3 may not be fitted correctly. If this is the case, iteratively
602 increasing the window length of the smoothing SAVGOL filter[34] solves this issue.

603

604 6.6.13 Once the analysis is finished, click on **ES** in the **Save** box. This will export a .tsv file in
605 the specified directory, containing the average elasticity as a function of the average
606 indentation depth and contact radius, the metadata associated with the experiment (see
607 above), and the estimated model parameters explained above. Finally, report the average
608 elasticity (disregarding the dependency on *δ*) and its SD.

609

610 6.6.14 Close the software and input the saved results in any other software of preference to

611 <mark>further plot the data and perform statistical analysis.</mark>
612
613 NOTE: This step is optional: Export graphs from the GUI by right-clicking on the graph and
614 selecting **Export**. Export the graph in .svg, so that parameters such as font, font size, line style,
615 etc. can be edited in another software of choice. Custom CP algorithms and filters can be
616 programmed and added to the already existing ones. See **Supplementary Note 1** for details.
617
618 **REPRESENTATIVE RESULTS**:
619 Following the protocol, a set of *F-z* curves is obtained. The dataset will most likely contain
620 good curves, and curves to be discarded before continuing with the analysis. In general,
621 curves should be discarded if their shape is different from the one shown in **Figure 4A**. **Figure**
622 **5AI** shows a dataset of ~100 curves obtained on a soft PAAm hydrogel of expected *E* 0.8 KPa[35]
623 uploaded in the NanoPrepare GUI. Most curves present a clear, flat baseline, a transition
624 region, and a sloped region that is proportional to the apparent stiffness of the material[13].
625 However, a minority of curves show alterations from the shape shown in **Figure 4A**, such as
626 the absence of a baseline, missed contact, or a sloped baseline. These curves can be easily
627 removed from the dataset using NanoPrepare (**Figure 5AII**, red curves), and a clean dataset
628 can be saved in the standard JSON format (**Figure 5AIII**). The clean dataset is uploaded in
629 NanoAnalysis (**Figure 5BIV**), which has been designed so that it batch processes all curves.
630 This means each step of the workflow is applied to the whole dataset. After being uploaded,
631 curves can be filtered to remove random noise using one or more filters described in the
632 **Discussion** section (**Figure 5BV**). The CP is then located using one of the algorithms
633 implemented in the software and detailed in the **Discussion** (**Figure 5BVI**). Once the CP has
634 been identified, *F-z* data is converted into *F-δ* data. Because the software has been designed
635 to primarily analyze data from ferrule-top nanoindentation devices based on optical fiber
636 sensing, which use probes having a spherical tip, the Hertz analysis is based on the Hertz
637 model approximating the contact between a sphere of radius *R* and an infinitely extended
638 linear elastic homogeneous isotropic (LEHI) half space[13]:
639
640 $$F = \frac{4}{3}\frac{E}{(1-v^2)}\delta^{\frac{3}{2}}R^{\frac{1}{2}} \quad (1)$$
641
642 where *F* is the force, δ is the indentation, *E* is Young's Modulus, and *v* is the Poisson's ratio,
643 taken as 0.5 assuming incompressibility. By fitting *F-δ* curves with equation 1, *E* can be
644 therefore estimated (see **Discussion**—critical steps in the protocol—for assumptions of the
645 Hertz model) (**Figure 5BVII**).
646
647 In addition to the Hertz analysis, the software can perform a more advanced analysis, namely,
648 the elasticity spectra, which is particularly useful for cell nanoindentation data; and can also
649 be used as a tool to estimate the influence of the underlying substrate on the mechanical
650 properties obtained *via* the Hertz model. Below, the approach is briefly summarized. Full
651 details can be found in the original publication[24].
652
653 Starting from the Oliver-Pharr model[36], which describes the indentation of an axisymmetric
654 punch of arbitrary geometry and an elastic half space, one can derive $E(\delta)$ for the specific
655 case of a spherical indenter. Taking *v* as 0.5, $E(\delta)$ has the form[24]:
656

657
$$E(\delta) = \frac{3}{8} \frac{1}{\delta\sqrt{R}} \frac{dF}{d\delta} \quad (2)$$

658

659 Computing $E(\delta)$ for each F-δ curve using equation 2 yields a set of curves, namely, the
660 elasticity spectra (ES). By taking the average of all curves in the data set, the average ES is
661 obtained (**Figure 5BVIII**). The average ES is a useful tool because it provides information on
662 how E varies with δ in the dataset. In the specific case of cell nanoindentation experiments,
663 the thickness of the cell is not known *a priori*, which means that choosing an appropriate
664 fitting range for the Hertz analysis is somewhat arbitrary. By using the average ES, substrate
665 effects on the apparent $E(\delta)$ become evident, which means the tool can be used to select an
666 appropriate fitting range, corresponding to the point where $E(\delta)$ starts increasing after its
667 decay. Further, it has been previously demonstrated and computationally and experimentally
668 validated that a simple bilayer model is effective in the estimation of the actin cortex's
669 thickness (d_0), the actin cortex's modulus (E_0), and the cell's bulk modulus (E_b)[24]. The model
670 describes the cell as a bilayer, with an outermost layer of thickness d_0 and modulus E_0, and an
671 inner layer of infinite thickness with elastic modulus $E_b < E_0$:

672

673
$$E(\delta) = E_b + (E_0 - E_b)e^{-\left(\frac{\Lambda\sqrt{R\delta}}{d_0}\right)} \quad (3)$$

674

675 where R is the tip's radius and Λ is a phenomenological parameter, which was determined to
676 be 1.74 from finite element analysis simulations[24]. This procedure has been implemented in
677 the NanoAnalysis software, which allows to fit the average ES with equation (3) to obtain an
678 estimate of E_0, E_b, and d_0 (**Figure 5BVIII**, black dashed line). For full methodological details,
679 refer to the original publication[24].

680

681 To demonstrate the viability of the protocol, the elasticity of PAAm hydrogels of known E
682 (measured by AFM)[35] were prepared and tested using the procedure suggested in Part 1 of
683 the protocol. For each gel, two stiffness maps in two different areas of the sample were
684 acquired using a commercial ferrule-top nanoindenter equipped with a tip having R = 52 μm
685 and k = 0.46 N/m. Each map consisted of 50 indentations performed in displacement control,
686 and the step size in x and y was set to 20 μm to avoid oversampling. **Figure 6A** shows the
687 average F-δ curve together with the average Hertz model for a soft PAAm hydrogel (expected
688 E 0.8 kPa) and a stiff PAAm hydrogel (expected E 8 kPa)[35]. By performing the Hertz analysis
689 through the NanoAnalysis software and plotting individual values of E, the expected E was
690 retrieved for both hydrogels (**Figure 6B**).

691

692 Further, nanoindentation experiments on HEK293T cells were performed. Seven individual
693 cells were indented by performing a matrix scan with x and y step size set to 0.5 μm on each
694 cell and acquiring a minimum of 25 curves on each cell. This resulted in the analyzed dataset
695 containing ~200 curves. The selected probe had R = 3.5 μm and k =0.02 N/m.

696

697 **Figure 7A** shows the average Hertz curve and the corresponding average Hertz model, plotted
698 using the mean E obtained from fitting equation (1) to each individual curve in NanoAnalysis
699 up to an indentation of 200 nm. E was found to be 915 ± 633 Pa, which is in accordance with
700 values reported in the literature[24]. Despite its wide use, the Hertz model does not fully capture
701 the evolution of the force with increasing indentation depth for cell nanoindentation

experiments (**Figure 7A**). Because of this, the ES is a particularly suitable tool to study the mechanical properties of single cells.

Figure 7B shows the average ES, together with equation (3) fitted up to an indentation of 200 nm. The average ES starts increasing at an indentation depth of ˜200 nm, which indicates the contribution of the substrate to the probed apparent E (**Figure S4**). Because of this, 200 nm was chosen as the fitting range for both the Hertz model (**Figure 7A**) and the bilayer model (**Figure 7B**). Fitting equation (3) to the average ES allowed to extract important information, which would otherwise remain inaccessible from simple nanoindentation experiments analyzed using the Hertz model. Specifically, the actin cortex's modulus (E_0) was estimated to be 5.794 ± 0.095 kPa, the actin cortex's thickness (d_0) was found to be 311 ± 3 nm and the bulk modulus (E_b) was found to be 0.539 ± 0.002 kPa. All values are in accordance with previous experiments performed using AFM on the same cell type[24], and with values that have been reported in the literature[37,38]. Specifically, the actin cortex is expected to be between 300–400 nm for adherent cells[37], and up to 10 times stiffer than the bulk of the cell[38].

Regardless of the bilayer model, a direct comparison between results obtained with the standard Hertz model and the ES approach is given in **Figure 7C**, which reveals overlapping distributions with comparable means.

FIGURE AND TABLE LEGENDS:

Figure 1: Protocol overview. The protocol consists of the following parts: (**A**) Part 1: Preparing the sample (either hydrogels or cells) for nanoindentation experiments. (**B**) Part 2: Choosing the right probe and calibrating the probe. (**C**) Part 3: Performing nanoindentation experiments by acquiring stiffness maps on the sample. (**D**) Part 4: Analyzing the data, which consists of i) cleaning the acquired dataset through the first GUI (NanoPrepare) and saving the cleaned dataset and associated metadata as a standard JSON file; and ii) analyzing the cleaned dataset in the second GUI (NanoAnalysis), which consists of data filtering, CP identification, and model fitting to estimate Young's modulus E of the sample. Results are saved for further plotting and statistical analysis, which can be performed in any software of choice.

Figure 2: Sample preparation. (**A**) Steps suggested to prepare flat PAAm hydrogels for nanoindentation experiments. These are: i) pouring the hydrogel solution onto a hydrophobic glass slide and covering it with a silanized coverslip; ii) waiting for 20 min for polymerization to occur and peeling off the coverslip-gel composite from the glass slide; and iii) attaching the coverslip-gel composite to a Petri dish and adding appropriate solution (purified water in the context of this protocol) for nanoindentation experiments. The same rationale can be adapted and applied to any other type of hydrogel. (**B**) Steps suggested to prepare cells for nanoindentation experiments. These are: i) seeding cells and waiting for cell adhesion; ii) serum starving the cells to synch the cell population in terms of the cell cycle (optional); and iii) waiting for cells to be in an adhered state at desired confluency before starting nanoindentation experiments.

Figure 3: Nanoindentation probe overview and selection. (**A**) Schematic of ferrule-top probe (left) and picture of a ferrule-top probe with the spherical tip of radius 250 μm (right). All components are labeled in the photo. (**B**) Enlarged schematic of the cantilever and the spherical tip. The cantilever is treated as a Hookean spring of elastic constant k (shown at an

749   angle for representation purposes). The tip is defined by its radius, R. When the sample is
750   indented, the probe is displaced by an amount z from its reference position z_0, which results
751   in the cantilever bending d from its reference bending d_0. A force of $F = k\,(d - d_0)$ is applied
752   to the sample, which results in an indentation $\delta = (z - z_0) - (d - d_0)$. (**C**) Cantilever's
753   stiffness k should be chosen according to the expected elasticity of the substrate. The plot
754   was obtained considering Hertzian contact with an indentation of 1 µm, assuming that the
755   energy is equally shared between the cantilever's bending and the substrate's indentation
756   (i.e., $d = \delta$). The larger the tip radius, the stiffer the cantilever should be to reach the same
757   indentation for a substrate with a given E.

758

759   **Figure 4**: **Morphological characteristics of *F-z* curves.** (**A**) Successful experiment results in the
760   approach segment of an *F-z* curve having a clear baseline (tip approaching the sample but not
761   in contact); a transition region where the tip first contacts the sample; and a region where
762   the force increases with the displacement, where the tip is progressively indenting the
763   sample. The slope of this region is proportional to the apparent stiffness of the material[13],
764   meaning that curves belonging to stiff biomaterials (e.g., highly crosslinked gels) will be
765   steeper than those belonging to softer biomaterials (e.g., weakly crosslinked gels and cells).
766   (**B**) An approach curve where the tip never entered contact with the sample. See
767   troubleshooting of the method in the **Discussion** for resolution. (**C**) An approach curve where
768   the tip started in contact with the sample. See troubleshooting of the method in the
769   **Discussion** for resolution. The data shown is from an experiment performed on a soft PAAm
770   hydrogel of expected E 0.8 kPa[35].

771

772   **Figure 5: Data analysis workflow using the Python GUIs.** (**A**) An example dataset of *F-z* curves
773   acquired using a commercially available ferrule-top nanoindenter on a soft PAAm hydrogel
774   (expected E 0.8 kPa[35]) was uploaded in NanoPrepare. Curves that do not follow the shape
775   described in **Figure 4A** are excluded from the dataset, and the clean dataset and associated
776   metadata are saved as a standard JSON file. (**B**) The clean dataset is uploaded in the second
777   GUI (NanoAnalysis) where curves can be filtered by applying one or more filters to remove
778   noise (see **Discussion**, critical steps in the protocol). Further, a CP algorithm is selected to
779   automatically locate the CP for all curves (see **Discussion**, critical steps in the protocol). The
780   Hertz analysis is then performed, yielding a $F-\delta$ curve for each indentation, which is fitted
781   with the Hertz model to yield a scatter plot of E. The obtained results can be saved for further
782   plotting. For cells, an additional analysis called the elasticity spectra[24] can be performed. All
783   graphs shown were directly exported from both NanoPrepare and NanoAnalysis GUIs. Details
784   for each step of the workflow are given in the main text.

785

786   **Figure 6: Elasticity of PAAm hydrogels.** (**A**) Average $F-\delta$ curve from a set of ~100 curves
787   acquired on a soft PAAm hydrogel (expected E 0.8 kPa[35]) and a stiff PAAm hydrogel (expected
788   E 8 kPa[35]). The shaded band shows one standard deviation (SD). The dashed line shows the
789   Hertz model plotted using the average E from the NanoAnalysis software, obtained by fitting
790   the Hertz model to each curve up to a maximum indentation of 2,000 nm (~4% of R, R = 52
791   µm, k = 0.46 N/m). Curves were smoothed using the prominecy filter with default parameters,
792   and the CP was identified using the RoV algorithm[32]. (**B**) Individual values of E were obtained
793   from the analysis performed in NanoAnalysis plotted for statistical comparison. The raincloud
794   plot was obtained using the Python module described in reference[39]. **** $p < 0.0001$, two-
795   tailed unpaired *t*-test, α=0.05.

796
797 **Figure 7: Elasticity of HEK cells.** (**A**) Average $F-\delta$ curve from a set of ˜200 curves acquired on
798 six individual HEK cells. The shaded band shows one SD. The dashed line shows the Hertz
799 model plotted using the average E computed using the NanoAnalysis software, obtained by
800 fitting the Hertz model to each curve up to a maximum indentation of 200 nm (˜6% of R, R =
801 3.5 µm, k = 0.02 N/m). Curves were smoothed using the prominecy filter with default
802 parameters and a SAVGOL filter[34] with order 3 and window length 80 nm, and the CP was
803 identified using the threshold algorithm[33]. Using the Hertz model, the cell is treated as a
804 homogeneous sphere with Young's Modulus E, as schematically shown in the inset (the
805 nucleus is depicted for pictorial purposes). (**B**) Average elasticity spectra computed on the
806 same data set described in (A). By fitting a bilayer model to the average elasticity spectra,
807 estimations of the actin cortex modulus (E_0), the cell's bulk Young's modulus (E_b), and the
808 actin cortex's thickness (d_0) are computed. For the dataset shown: E_0 = 5.79 ± 0.09 kPa, E_b =
809 0.539 ± 0.002 kPa and d_0 = 311 ± 3 nm. (**C**) Comparison between the Hertz model and the
810 elasticity spectra approach in terms of E distribution. For the elasticity spectra, the
811 distribution represents the values of E from the average elasticity spectra, regardless of
812 indentation depth (up to a maximum indentation of 200 nm). The continuous lines
813 superimposed on the histograms are Gaussian kernel density estimates of the underlying
814 distributions. E = 915 ± 633 Pa (Hertz) and E = 890 ± 297 Pa (elasticity spectra).
815
816 **Figure S1: Calibration Procedure.** (**A**) Successful wavelength scan. The deflection and
817 displacement signals during the wavelength scan (left). The sinusoidal wave on the
818 interferometer's screen at the end of the wavelength scan (right). (**B**) Find surface procedure.
819 Deflection and displacement signals as the probe is lowered in 1 µm steps after contact with
820 a stiff substrate. (**C**) Geometrical factor calibration. During indentation of a stiff substrate, the
821 deflection follows the displacement (green and blue lines). The indentation should be
822 approximately zero (red line). If the deflection lags the displacement in time (green dashed
823 line), the probe is not fully in contact with the stiff substrate. (**D**) Demodulation signal. The
824 demodulation signal on the interferometer's screen at the end of the calibration procedure
825 (left) and when tapping on the nanoindenter (right).
826
827 **Figure S2: NanoPrepare GUI.** Screenshots of the NanoPrepare GUI. Details on the
828 functionality of each widget are given in the main **Protocol** and the **Discussion**.
829
830 **Figure S3: NanoAnalysis GUI.** Screenshots of the NanoAnalysis GUI. Details on the
831 functionality of each widget are given in the main **Protocol** and the **Discussion**.
832
833 **Supplementary Note 1: Adding custom filters and CP algorithms to the NanoAnalysis**
834 **software.**
835
836 **Figure S4: Depth dependency of average elasticity spectra.** The plot shows the average
837 elasticity spectra $<E(\delta)>$ (solid red line) together with one standard deviation ($\sigma(E(\delta))$. After
838 an initial decay, the average elasticity spectra start increasing, which is mainly associated with
839 the effects of the stiff underlying substrate on the probed apparent elastic modulus. The
840 maximum indentation depth used to fit the Hertz model to $F-\delta$ curves, and the decay model
841 to the average elasticity spectra should be chosen so that the underlying substrate does not
842 affect the results (Fit range).

843
844 **DISCUSSION:**
845 This protocol shows how to robustly acquire force spectroscopy nanoindentation data using
846 a commercially available ferrule-top nanoindenter on both hydrogels and single cells. In
847 addition, instructions for the use of an open-source software programmed in Python
848 comprising a precise workflow for the analysis of nanoindentation data are provided.
849
850 Critical steps in the protocol
851 The following steps have been identified to be of particular importance when following this
852 protocol.
853
854 Sample preparation: It is crucial that before initiating measurements, the sample is prepared
855 with the restraints of the measurement in mind. That is, the sample must be adhered to a
856 surface and be as flat as possible. This is especially important when preparing samples that
857 do not naturally adhere to surfaces as cells do, such as hydrogels. Firstly, the sample must not
858 float in solution as this will interfere with measurements and potentially damage the probe.
859 For this, chemical functionalization of a coverslip is recommended, so that the hydrogel can
860 be polymerized adhered to a surface, which can later be glued to a Petri dish while
861 submerged. Moreover, the sample's surface must be as flat as possible to ensure coherent
862 surface detection by the probe and avoid damaging the probe while moving in x and y during
863 a matrix scan. The hydrogel solution can be polymerized on a hydrophobic glass slide, which
864 makes the resulting hydrogel flat without adhering to it. If these considerations are not
865 followed, it will be difficult to obtain clean F-z data.
866
867 In the case of cell preparation, it is best to indent cells with similar morphology to improve
868 data homogeneity. In the event that cells grow in a heterogeneous population, a serum
869 starvation step can be introduced pre-measurement, to aid cell cycle synchronization and,
870 therefore, remove potential experimental confounders[40,41]. In the case of non-adherent cells
871 or organoid cultures, one must perform extra steps to ensure stability and adherence of the
872 biological sample while measurements are being performed. Extra steps might include
873 chemically binding cells to culture plates or using tissue adhesives that are now widely
874 commercially available.
875
876 Nanoindentation experiments: It is important that a cantilever with the right k is chosen
877 depending on the sample's expected E[15]. This is because if the cantilever is too stiff, the
878 sample will be indented but no significant cantilever bending will occur. Conversely, if the
879 cantilever is too soft with respect to the sample, the cantilever will excessively bend with
880 minimal indentation. Both instances will result in the miscalculation of E in the subsequent
881 analysis.
882
883 For probe calibration, the probe must be wet prior to insertion into the calibration dish to
884 minimize surface tension when encountering the liquid of the calibration dish. Not doing so
885 may cause the trapping of air bubbles or push the cantilever against the optical fiber. This can
886 also result in the probe being damaged.
887
888 The use of a thick glass Petri dish is recommended for calibration. Glass is infinitely stiff
889 compared to the cantilever, which allows accurate calibration of the cantilever's k while

890   indenting the glass. Further, the weight of the glass ensures a stable substrate that is more
891   robust against noise (e.g., airflow and acoustic vibrations) compared to a lighter plastic Petri
892   dish. The calibration performs a linearization procedure of the interferometric signal
893   measured at the detector (V/t), which means the signal will be converted into linear cantilever
894   bending (µm/t) using the unit circle (demodulation circle) as a linearization tool[18]. The
895   deflection sensitivity (µm/V) is set by default in the interferometer and used to convert V to
896   µm. During this procedure, the calibration factor is also determined, which originates from
897   the mismatch in position between the spherical tip and the fiber position where the signal
898   read-out occurs (**Figure 3A**). By indenting on a stiff substrate-like glass, the deflection
899   measured by the fiber is approximately the same as the distance displaced by the piezo, which
900   means the indentation depth is approximately zero. Taking their ratio yields the calibration
901   factor. It is important that the calibration of the instrument is performed correctly, and that
902   all checks are satisfied before continuing to acquire *F-z* data.

904   When configuring an indentation profile, it is useful to keep in mind the assumptions of the
905   Hertz model, which will be used later to analyze the data. The Hertz model is derived assuming
906   that the sample is a linear elastic homogeneous isotropic (LEHI) infinitely extended half-space,
907   which results in the following practical consequences: i) applied strains should not exceed
908   20% (as a rule of thumb, the δ should not exceed 10% of the tip's R) and ii) δ should be less
909   than 10% of the sample thickness, and small compared to the other sample's dimensions[13].

911   The maximum displacement (or indentation depth/force depending on the operation mode)
912   can be adjusted depending on the resulting δ, and whether surface or bulk mechanical
913   properties are desired. If the sample has been indented to a slightly larger δ, the Hertz model
914   can still be fitted up to a maximum δ, which lies within its assumptions in the NanoAnalysis
915   software, and the average ES used to estimate this range (see **Representative Results**).

917   For cell nanoindentation experiments, it is challenging to perform multiple matrix scans on
918   the same cell. However, if the cell is large enough, it may be possible to find another suitable
919   region and repeat the procedure on the same cell, for example, an experiment where the user
920   wants to detect differences in the mechanical properties of a certain region of the cell
921   compared to another. Usually, a map per cell is performed, and a minimum of five cells are
922   indented per biological condition. It is advisable to repeat the experiment at least three times
923   so that sufficient data is acquired on each sample (i.e., three replicates for each cell biological
924   condition).

926   Critically, acquired curves should present a flat baseline, a transition region, and a sloped
927   region. Curves that do not present a baseline cannot be later analyzed due to uncertainty on
928   the location of the CP. If curves deviate from the shape shown in **Figure 4A**, the contact
929   threshold should be optimized before continuing with the experiment (see troubleshooting
930   of the method below).

932   Sufficient data should be acquired to ensure statistically robust results, given the nature of
933   the technique, which probes mechanical properties locally.

935   Data analysis: The software described in this protocol is routinely adopted to analyze
936   nanoindentation data and it has been used to obtain results published in several peer-

937 reviewed journals (e.g., nanoindentation of hydrogels[8,21], nanoindentation of cells[24,42]).
938 Analysis of nanoindentation data is non-trivial. It is suggested to pay particular attention to
939 the following parts:
940
941 Screening of the dataset: The dataset should be thoroughly screened in the NanoPrepare
942 software, and all unsuccessful curves should be removed before saving the cleaned dataset
943 as a JSON file. Curves can still be excluded from the analysis in the NanoAnalysis software, but
944 the JSON file cannot be changed. As such, to ensure consistency between the cleaned and
945 analyzed dataset, it is suggested to carefully perform the screening process in the
946 NanoPrepare software.
947
948 Filtering data: Using filters is useful when the data is noisy and recommended when
949 performing the ES analysis. Three major filters are used as described below.
950
951 Prominency: This filter removes prominent peaks in the Fourier space, to eliminate
952 instrumental oscillations typical of commercially available ferrule-top nanoindenters. The
953 filter is based on three parameters: Prominency (a.u.): the peak prominency in the Fourier
954 space; Minimum frequency (channels): the minimum frequency to be filtered; Band (% of
955 peak position): the width around the filtered frequency in percentage of the peak position.
956 Activate this filter for data originating from commercially available ferrule-top nanoindenters
957 by clicking on the checkbox and leaving default parameters.
958
959 Savitzky Golay (SAVGOL), algorithm from the SciPy library[34] (scipy.signal.SAVGOL_filter): This
960 filter smooths the data based on a local least-squares polynomial approximation. Activate this
961 filter if the data is particularly noisy. Change the order of the polynomial and the filter window
962 length in the GUI depending on how noisy the data is. For more details, see references[30,31].
963 Activate this filter for the ES analysis.
964
965 Median filter, algorithm from the SciPy library[34] (scipy.signal.medfilt): This filter smooths the
966 data based on replacing each point with the median calculated around that point in a given
967 window. Change the window length in the GUI depending on how noisy the data is. This filter
968 is used as an alternative to the SAVGOL filter.
969
970 Activating the prominency filter helps remove instrumental noise (low-frequency oscillations)
971 typical of commercial ferrule-top nanoindenters. In general, activating other filters such as
972 the SAVGOL[34] when performing the simple Hertz analysis is not necessary. When computing
973 the ES, it is recommended to activate both the prominency filter and the SAVGOL filter[34], with
974 a smoothing window depending on the level of noise present in the data. This is because the
975 ES contains a derivative term (equation 2), which is very sensitive to noise. For example,
976 results in **Figure 7** were obtained using the prominency filter together with a SAVGOL filter[34]
977 with window 80 nm and polynomial order 3. However, it is important not to over smooth the
978 data, because this may hide any differences that are present between datasets.
979
980 CP identification: The most important part of the analysis is the identification of the CP, which
981 strongly influences both the absolute value of E and its distribution[32,33]. Four algorithms based
982 on automatic search procedures that locate the CP in order to remove human bias have been
983 implemented in the NanoAnalysis software. All algorithms are based on automatic search

984   procedures that have been documented in the literature[32,33]. In general, every point in a
985   region of interest is tested as a trial CP while an algorithm-specific parameter is being
986   computed. The point that returns the optimized parameter, which can be its maximum or
987   minimum value depending on the algorithm, is taken as the CP[32]. Those procedures have been
988   implemented to remove human bias and take a statistical approach to the problem. Because
989   each algorithm computes the CP based on the optimization of a given parameter, the
990   identified CP will be slightly different for each algorithm. As such, it is paramount to maintain
991   the same CP algorithm and specific parameters (e.g., window length for the RoV algorithm)
992   between datasets that one wants to compare, as relative differences in E will be preserved.
993   The different CP algorithms and their parameters are summarized below.

995   Goodness of Fit (GoF): An approach based on fitting a contact mechanics model (Hertz) from
996   each *(z, F)* pair in a region of interest and selecting the fit having the highest R^2 value. It works
997   well where the transition between non-contact and contact is evident, which happens with
998   stiff materials such as highly crosslinked hydrogels. The algorithm is computationally
999   expensive, and generally the slowest. Here, it has been implemented so that the Hertz model
1000   is only fitted up to a maximum δ of about 10% of R, as this has been shown to yield more
1001   accurate results[32].

1003   Ratio of Variances (RoV): An approach based on computing the ratio of the variance of the
1004   deflection (force) signal in the non-contact and contact region[32].

1006   Second derivative: An approach based on the second derivative of the deflection (force)
1007   signal[33]. It works well when the signal is clean. If the signal is too noisy, this approach is not
1008   recommended.

1010   Threshold: An approach based on the average deflection (force) in the noncontact region[33].
1011   In short, starting from a force value selected by the user near the contact region, the
1012   algorithm iterates through each point toward the baseline, until it finds the first point whose
1013   force value is larger than the average of the baseline. This point is selected as the CP. This
1014   algorithm is very robust and is the recommended one to use.

1016   Details on how to use each algorithm are given below. The CP algorithms involve numerical
1017   constants that need to be changed in the GUI to suit the specific dataset. Specifically, the
1018   following parameters are common to the GoF, the RoV, and the second derivative method,
1019   allowing to select a sub-region of the curves (region of interest or ROI) where the CP will be
1020   searched for.

1022   Safe threshold (nN): It defines the maximum force in nN (and the corresponding *z* point) from
1023   which the CP will be searched. This is the right boundary of the ROI, whose default value is 10
1024   nN. All curves whose maximum force is below this threshold will be automatically moved to
1025   the failed set. Change this value to a force value slightly above the transition from non-contact
1026   to contact.

1028   X range (nm): It defines the range in nm from the *z* point corresponding to the safe threshold.
1029   This is the left boundary of the ROI. The default of 1,000 nm is a good starting point, but if the
1030   CP is found too late in the curve (i.e., in the sloped region), increase this value. Conversely, if

1031   the CP is found too early (i.e., in the baseline), decrease this value.

1032

1033   Parameters specific to each algorithm are summarized here. For the GoF, the Window Fit (nm)
1034   represents the window in nm from the trial CP up to which the Hertz model is fitted. This is
1035   capped at a value of 10% of R. For the RoV, the Window RoV (nm) represents the window in
1036   nm to the left and right of the trial CP over which the variance of the deflection (force) signal
1037   is computed. For the second derivative, the Window P (nm) represents the window passed to
1038   the SAVGOL filter[34] used to compute the second derivative of the deflection (force) signal.
1039   Default values have been set from testing the different algorithms and it is generally not
1040   required to change them.

1041

1042   For the threshold algorithm, the following parameters can be changed:

1043

1044   Align threshold (nN): The force (F_0) from which the CP will be looked for starting from this
1045   point and moving toward the baseline. All curves whose maximum force is below this
1046   threshold will automatically be moved to the failed set. Its default value is 10 nN; however,
1047   change this value to a force value slightly above the transition from non-contact to contact.
1048   The corresponding z point (z_0) is stored for later use in the algorithm (see below).

1049

1050   Align left step (nm): This parameter defines the shift to add to the left of z_0 (default value
1051   2,000 nm), which results in the calculation of a point defined by (z_0 - align left step). This point
1052   is the point around which the average of the baseline will be computed (see below).

1053

1054   Average area (nm): This parameter defines the average area to the left and right of (z_0 - align
1055   left step), over which the average of the baseline will be computed. Its default value is 100
1056   nm, and it is not required to change it.

1057

1058   Iterating down from F_0, the CP is taken as the first point whose value is above the force
1059   defined by the average of the baseline.

1060

1061   Note on the ES and noise: The average ES may appear noisy at first with prominent sinusoidal
1062   oscillations, and as a result equation 3 may not fit correctly. If this is the case, increasing the
1063   window of the smoothing SAVGOL filter[34] usually solves this issue.

1064

1065   Modifications and troubleshooting of the method

1066

1067   Troubleshooting of the method

1068

1069   Wavelength scan troubleshooting
1070   If an error message appears on the interferometer's display after performing the wavelength
1071   scan, the following problems may be the cause: i) The environment may be contaminated by
1072   noise. Get rid of any noise sources, including airflow, loud noises, and mechanical vibrations;
1073   ii) The probe may not be properly connected. Unplug and re-plug the green optical fiber
1074   connector; iii) The cantilever may be dirty. Clean it by submerging the probe in a Petri dish
1075   containing isopropanol for a few minutes, and then H_2O; iv) An air bubble may be present on
1076   the cantilever. Submerge the probe in a Petri dish containing isopropanol and create some
1077   flow by pipetting the liquid up and down; v) The cantilever may be bent/stuck to the fiber,

1078 which can be seen under the microscope. Release it by gently touching the cantilever with a
1079 tissue wipe. Take extra care when touching the cantilever as the application of excessive force
1080 can break it; vi) The cantilever is missing from the probe, which can be seen under the
1081 microscope. The only solution is using a new probe. Try the wavelength scan again, which
1082 should now be successful.
1083
1084 Calibration troubleshooting
1085 If calibration fails and the new factor is either NaN or is not in the expected range, the
1086 following problems may be the cause: i) The tip is not fully in contact with the substrate. Make
1087 sure the tip is in contact with the substrate by following the steps given in the **Protocol**; ii)
1088 Attractive forces between the tip and the glass surface (snap-on behavior) result in the
1089 calibration of the over-bended cantilever. Clean the probe by submerging it in isopropanol for
1090 5 min. Clean the dish with isopropanol; iii) The tip/dish may be contaminated: clean the probe
1091 by submerging it in isopropanol for 5 min. Clean the dish with isopropanol; iv) The cantilever
1092 may be bent/stuck to the fiber. Release it by gently touching it with a tissue wipe. Repeat
1093 both wavelength scan and calibration after troubleshooting.
1094
1095 Contact troubleshooting
1096 If curves deviate from the shape shown in **Figure 4A**, experimental parameters need to be
1097 adjusted before continuing with the experiment. Two of the most common problems are:
1098
1099 An approach curve where the tip never enters contact with the sample (**Figure 4B**). This occurs
1100 when the contact threshold is set to a value that is too low, and noise causes the cantilever
1101 to bend by an amount corresponding to the given threshold. To solve this issue, navigate to
1102 the **Options** menu and slowly increase the threshold at steps of 0.01 and perform an
1103 indentation until the curve resembles the one shown in **Figure 4A**. Decreasing the speed in
1104 the same menu can also help solve this issue.
1105
1106 An approach curve where the tip started in contact with the sample (**Figure 4C**). This happens
1107 when the contact threshold is set to a value that is too high, and the cantilever does not bend
1108 by the amount corresponding to the given threshold when first touching the sample. To solve
1109 this issue, slowly decrease the threshold in the **Options** menu at steps of 0.01 and perform an
1110 indentation until the curve resembles the one shown in **Figure 4A**. This issue is particularly
1111 problematic because the absence of a baseline prevents the correct computation of the CP,
1112 eventually leading to a miscalculation of *E*.
1113
1114 Modifications of the method
1115 The protocol can be extended to quantify the *E* of different types of hydrogels. PAAm
1116 hydrogels were chosen for this protocol as they are the most common hydrogels used within
1117 the field of mechanobiology. However, the protocol is equally applicable to any type of elastic
1118 hydrogel[25], both synthetic, for example, polyethylene-glycol (PEG)[43] and gelatin methacryloyl
1119 (GelMA)[44,45]; and natural, such as collagen[46]. Moreover, there are no constraints on the
1120 dimensions of the sample to test, within reasonable limits. For example, this protocol has
1121 been used to quantify the *E* of synthetic PEG that was later tested using a bulk rheometer and
1122 required to be ~15 mm in diameter and ~2 mm in thickness[8]. The protocol has also been
1123 implemented to characterize the *E* of PDMS membranes that were polymerized in a Petri dish
1124 (results not published).

1125

1126 Besides standard indentation of single cells performed using a conventional inverted phase-
1127 contrast microscope, ferrule-top nanoindenters are compatible with complex imaging
1128 systems and have been used to probe the local elasticity subcellular structures, such as the
1129 cell's nucleus and cytoplasm[47]. Whereas steps will need to be adjusted depending on the
1130 specific optical system, this protocol is of general applicability with respect to performing
1131 nanoindentation experiments and analyzing the resulting data.

1132

1133 Further, the protocol is not limited to measuring the mechanical properties of cells and
1134 hydrogels and can be adapted to measure the local elastic properties of more complex
1135 systems, including organoids[48], spheroids[49], and whole tissues such as kidneys, liver, spleen,
1136 and uterus[23]. The reader is directed to references[23,48,49] for specificities on performing
1137 nanoindentation experiments on such samples. One aspect to consider is that displacement
1138 control works in open-loop mode and does not receive feedback from the sample. As such,
1139 constant stress/strain and speed are not ensured, and softer parts of the sample will be
1140 indented more and faster as compared to stiffer regions. This is relevant for mechanically
1141 heterogeneous samples such as tissues, where it is more appropriate to choose either
1142 indentation control (I mode) or load control (P mode), ensuring a consistent stress/strain and
1143 speed across mechanically heterogeneous regions of the sample.

1144

1145 Limitations of the method
1146 There is a growing body of evidence that viscoelasticity, in addition to elasticity, plays an
1147 important role in regulating physiologically and pathologically relevant processes. This is
1148 because cells, the ECM, and tissues are viscoelastic, and elasticity represents only one
1149 component of their mechanical behavior[50–53]. Whereas ferrule-top nanoindenters provide
1150 functionality for characterizing viscoelasticity, including stress relaxation, creep compliance,
1151 and dynamic mechanical analysis to extract both the storage and loss modulus over different
1152 frequency (time) regimes, this protocol only focuses on elasticity, which remains the most
1153 studied mechanical variable in the context of mechanobiology and tissue engineering (for
1154 example, see reference[3]).

1155

1156 The underlying assumption with consequences on both experiments and data analysis is that
1157 the indented substrate behaves as a linear elastic homogeneous isotropic (LEHI) solid. This
1158 means that the stress-strain response is linear, there are no time-dependent behaviors, and
1159 the sample is mechanically homogeneous and isotropic. Based on these assumptions, the
1160 mechanical properties of the substrate are quantified through Young's modulus *(E)* following
1161 a specific contact mechanics model, in this case, the Hertz model (equation 1). For small quasi-
1162 static forces/deformations, chemically crosslinked hydrogels such as PAAm gels used in this
1163 protocol[35] behave nearly as elastic solids and viscoelastic effects are minimal and negligible[53].
1164 On the other hand, cells are not LEHI solids and show complex mechanical behavior[9]. The
1165 Young's modulus of cells is highly dependent on the strain rate (i.e., speed) of the indentation
1166 procedure, however, no clear trend is established and additional variables such as tip size and
1167 maximum indentation depth influence this relationship[9]. Nonetheless, for quasi-static
1168 deformations, such as those used in this protocol (v = 5 μm/s), cells show a marked elastic
1169 response and dissipative effects are minimal[9]. Strain rate dependency can be captured by
1170 more complex models taking into account time-dependent variables, to which the reader is
1171 referred to[54].

1172

1173 Further, following the same underlying assumption, the Poisson's ratio (ν) is taken as 0.5 both
1174 in the Hertz and ES analysis. When comparing between samples, this only impacts results as
1175 a coefficient; however ν has been shown to be a frequency-dependent quantity for cells[55] and
1176 to deviate from 0.5 for hydrogels[56].

1177

1178 Another limitation of the protocol lies in the fact that the software does not provide
1179 quantification of E through more sophisticated contact mechanics models. The Hertz model
1180 is the most used contact mechanics model in AFM experiments and it is extremely
1181 effective[13,15]; however, it does not take into account more complex events such as short- or
1182 long-range attractive forces between the tip and the sample. More complex models such as
1183 the Johnson-Kendall-Roberts model can capture these behaviors[13], but are not implemented
1184 in the software. For an overview of different contact mechanics models ranging in complexity,
1185 the reader is directed to reference[13].

1186

1187 Significance of the method with respect to existing/alternative methods
1188 The most common approach to quantify the local elastic properties of biomaterials and single
1189 cells at the microscale is AFM[13–16]. Despite being a powerful and versatile instrument, the
1190 AFM requires extensive training due to its complex setup before users can robustly perform
1191 experiments. Ferrule-top nanoindenters offer a plug-and-play solution while still allowing to
1192 apply nN forces with μm resolution to probe the local mechanical properties of biomaterials
1193 (e.g., references[8,19–21]). Whereas standardized protocols exist for the use of the AFM in the
1194 context of mechanobiology[16] and tissue engineering[14], there are no protocols detailing the
1195 operation of ferrule-top nanoindenter devices. This protocol allows an inexperienced user to
1196 perform nanoindentation experiments on both hydrogels and cells, by following guidelines
1197 that are intended to standardize the experimental workflow within the community. Further,
1198 data analysis of nanoindentation experiments is non-trivial and would remain largely
1199 inaccessible for users without experience in programming. Instructions are provided for the
1200 use of intuitive software that allows to clean and save the acquired dataset in light and
1201 standard format and perform both the standard Hertz analysis as well as the ES analysis[24] with
1202 a few clicks and in a reproducible way.

1203

1204 By following this protocol, results comparable with those obtained using the AFM are
1205 obtained, both for hydrogels' E (results in **Figure 6** compared to those in reference[35]) and
1206 cells' mechanical properties (results in **Figure 7** compared to those in reference[24]) at a fraction
1207 of the complexity. The method is of general applicability and can be adapted to different types
1208 of nanoindenters granted some steps are modified based on the specific device.

1209

1210 Importance and potential applications of the method in specific research areas
1211 Characterizing the elastic properties of cells, hydrogels, and tissues is standard practice in
1212 many research labs focusing on mechanobiology, tissue engineering/regenerative medicine,
1213 and beyond[3]. This protocol can be used to quantify the elastic properties of single cells,
1214 hydrogels, and adapted for tissues and more complex biomaterials in the context of
1215 physiologically relevant processes marked by a change in mechanical properties. For example,
1216 to mimic the dynamics of the native ECM, it has been shown that degradable 3D PEG-laminin
1217 hydrogels allow cells to remodel their surrounding environment, leading to a decrease in the
1218 gels' E of ~50% over a period of 9 days as compared to the same gels without cells[21]. The

protocol is of general applicability and is not restricted to the samples and optical setup described herein. It is envisaged that this protocol will facilitate the use of nanoindenters in research labs focusing on the study of mechanical properties in physiology and disease.

AUTHORS' CONTRIBUTIONS:
GC: software (contribution to software development and algorithms), formal analysis (analysis of nanoindentation data), validation, investigation (nanoindentation experiments on polyacrylamide gels), data curation, writing (original draft, review, and editing), visualization (figures and graphs). **MAGO:** investigation (preparation of gels and cells samples, nanoindentation experiments on cells), writing (original draft, review, and editing), visualization (figures and graphs). **NA:** validation, writing (review and editing). **IL:** software (contribution to software development and algorithms), validation, writing (review and editing); **MV:** conceptualization, software (design and development of original software and algorithms), validation, resources, writing (original draft, review, and editing), supervision, project administration, funding acquisition **MSS:** resources, writing (review and editing), supervision, project administration, funding acquisition. All authors read and approved the final manuscript.

REFERENCES:

1.   Dennis E. Discher, Paul Janmey, Y. W. Tissue cells feel and respond to the stiffness of their substrate. *Science (New York, N.Y.)*. **310** (5751), 1139–1143 (2005).
2.   Roca-Cusachs, P., Conte, V., Trepat, X. Quantifying forces in cell biology. *Nature Cell Biology*. **19** (7), 742–751 (2017).
3.   Guimarães, C. F., Gasperini, L., Marques, A. P., Reis, R. L. The stiffness of living tissues and its implications for tissue engineering. *Nature. Reviews. Materials*. **5**, 351–370 (2020).
4.   Moeendarbary, E., Harris, A. R. Cell mechanics: Principles, practices, and prospects. *Wiley Interdisciplinary. Reviews. Systems. Biology. and Medicine*. **6** (5), 371–388 (2014).
5.   Butcher, D. T., Alliston, T., Weaver, V. M. A tense situation: Forcing tumour progression. *Nature Reviews Cancer*. **9** (2), 108–122 (2009).
6.   Kubánková, M. et al. Physical phenotype of blood cells is altered in COVID-19. *Biophysical Journal*. **120** (14), 2838–2847 (2021).
7.   Engler, A. J., Sen, S., Sweeney, H. L., Discher, D. E. Matrix elasticity directs stem cell lineage specification. *Cell*. **126**, 677–689 (2006).
8.   Ciccone, G. et al. What caging force cells feel in 3D hydrogels: A rheological perspective. *Advanced. Healthcare. Materials*. **9** (17), e2000517 (2020).
9.   Wu, P. H. et al. A comparison of methods to assess cell mechanical properties. *Nature Methods*. **15** (7), 491–498 (2018).
10.   McKee, C. T., Last, J. A., Russell, P., Murphy, C. J. Indentation versus tensile measurements of young's modulus for soft biological tissues. *Tissue Engineering. Part B*

Reviews. **17** (3), 155–164 (2011).

11.   Humphrey, J. D., Delange, S. L. An Introduction to Biomechanics Solids and Fluids, Analysis and Design. Springer-Verlag, New York. 271–371 (2004).

12.   Prevedel, R., Diz-Muñoz, A., Ruocco, G., Antonacci, G. Brillouin microscopy: an emerging tool for mechanobiology. *Nature. Methods*. **16** (10), 969–977 (2019).

13.   Krieg, M. et al. Atomic force microscopy-based mechanobiology. *Nature Reviews Physics*. **1**, 41–57 (2019).

14.   Norman, M. D. A., Ferreira, S. A., Jowett, G. M., Bozec, L., Gentleman, E. Measuring the elastic modulus of soft culture surfaces and three-dimensional hydrogels using atomic force microscopy. *Nature Protocols*. **16** (5), 2418–2449 (2021).

15.   Gavara, N. A beginner's guide to atomic force microscopy probing for cell mechanics. *Microscopy Research and Technique*. **80** (1), 75–84 (2017).

16.   Whitehead, A. J., Kirkland, N. J., Engler, A. J. Atomic force microscopy for live-cell and hydrogel measurement. *Methods in Molecular Biology (Clifton, N.J.)*. **2299**, 217–226 (2021).

17.   Chavan, D. et al. Ferrule-top nanoindenter: An optomechanical fiber sensor for nanoindentation. *The Review of Scientific Instruments*. **83** (11), 115110 (2012).

18.   Van Hoorn, H., Kurniawan, N. A., Koenderink Ac, G. H., Iannuzzi, D. Local dynamic mechanical analysis for heterogeneous soft matter using ferrule-top indentation. *Soft Matter*. **12** (12), 3066–3073 (2016).

19.   Baldini, F. et al. Biomechanics of cultured hepatic cells during different steatogenic hits. *Journal of the Mechanical Behavior of Biomedical Materials*. **97**, 296–305 (2019).

20.   Emig, R. et al. Piezo1 channels contribute to the regulation of human atrial fibroblast mechanical properties and matrix stiffness sensing. *Cells*. **10** (3), 663 (2021).

21.   Dobre, O. et al. A hydrogel platform that incorporates laminin isoforms for efficient presentation of growth factors – Neural growth and osteogenesis. *Advanced Functional Materials*. **31** (21), 2010225 (2021).

22.   Antonovaite, N., Beekmans, S. V., Hol, E. M., Wadman, W. J., Iannuzzi, D. Regional variations in stiffness in live mouse brain tissue determined by depth-controlled indentation mapping. *Scientific Reports*. **8** (1), 12517 (2018).

23.   Wu, G., Gotthardt, M., Gollasch, M. Assessment of nanoindentation in stiffness measurement of soft biomaterials: kidney, liver, spleen and uterus. *Scientific Reports*. **10** (1), 18784 (2020).

24.   Lüchtefeld, I. et al. Elasticity spectra as a tool to investigate actin cortex mechanics. *Journal of Nanobiotechnology*. **18** (1), 147 (2020).

25.   Caliari, S. R., Burdick, J. A. A practical guide to hydrogels for cell culture. *Nature Methods*. **13** (5), 405–414 (2016).

26.   Blumlein, A., Williams, N., McManus, J. J. The mechanical properties of individual cell spheroids. *Scientific Reports*. **7** (1), 7346 (2017).

27.   Mirsandi, H. et al. Influence of wetting conditions on bubble formation from a submerged orifice. *Experiments in Fluids*. **61**, 83 (2020).

28.   Vassalli, M., Ciccone, G. CellMechLab/NanoPrepare: v0.1.1. Zendo (2021).

29.   Vassalli, M., Ciccone, G., Lüchtefeld, I. CellMechLab/nanoindentation: v1.0.0. Zendo (2021).

30.   Savitzky, A., Golay, M. J. E. Smoothing and differentiation of data by simplified least squares procedures. *Analytical Chemistry*. **36** (8), 1627–1639 (1964).

31.   Schafer, R. W. What is a savitzky-golay filter? in *IEEE Signal Processing Magazine*. **28** (4), 111–117 (2011).

1313   32.   Gavara, N. Combined strategies for optimal detection of the contact point in AFM
1314   force-indentation curves obtained on thin samples and adherent cells. *Scientific Reports*. **6**,
1315   21267 (2016).
1316   33.   Lin, D. C., Dimitriadis, E. K., Horkay, F. Robust strategies for automated AFM force
1317   curve analysis—I. Non-adhesive indentation of soft, inhomogeneous materials. *Journal of*
1318   *Biomechanical Engineering*. **129** (3), 430–440 (2007).
1319   34.   Virtanen, P. et al. SciPy 1.0: fundamental algorithms for scientific computing in Python.
1320   *Nature Methods*. **17** (3), 261–272 (2020).
1321   35.   Tse, J. R., Engler, A. J. Preparation of hydrogel substrates with tunable mechanical
1322   properties. *Current Protocols in Cell Biology*. Chapter 10 (2010).
1323   36.   Pharr, G. M., Oliver, W. C., Brotzen, F. R. On the generality of the relationship among
1324   contact stiffness, contact area, and elastic modulus during indentation. *Journal of Materials*
1325   *Research*. **7** (3), 613–617 (1992).
1326   37.   Kumar, R., Saha, S., Sinha, B. Cell spread area and traction forces determine myosin-
1327   II-based cortex thickness regulation. *Biochimica et Biophysica Acta - Molecular Cell Research*.
1328   **1866** (12), 118516 (2019).
1329   38.   Kunda, P., Pelling, A. E., Liu, T., Baum, B. Moesin controls cortical rigidity, cell rounding,
1330   and spindle morphogenesis during mitosis. *Current Biology: CB*. **18** (2), 91–101 (2008).
1331   39.   Allen, M., Poggiali, D., Whitaker, K., Marshall, T. R., Kievit, R. A. Raincloud plots: a
1332   multi-platform tool for robust data visualization. *Wellcome Open Research*. **4**, 63 (2019).
1333   40.   Clark, A. G., Paluch, E. Mechanics and regulation of cell shape during the cell cycle.
1334   *Results and Problems in Cell Differentiation*. **53**, 31–73 (2011).
1335   41.   Langan, T. J., Rodgers, K. R., Chou, R. C. Synchronization of mammalian cell cultures by
1336   serum deprivation. *Methods in Molecular Biology (Clifton, N.J.)*. **1524**, 97–105 (2017).
1337   42.   Hodgkinson, T. et al. The use of nanovibration to discover specific and potent bioactive
1338   metabolites that stimulate osteogenic differentiation in mesenchymal stem cells. *Science*
1339   *Advances*. **7** (9), eabb7921 (2021).
1340   43.   Kloxin, A. M., Kloxin, C. J., Bowman, C. N., Anseth, K. S. Mechanical properties of
1341   cellularly responsive hydrogels and their experimental determination. *Advanced Materials*
1342   *(Deerfield Beach, Fla.)*. **22** (31), 3484–3494 (2010).
1343   44.   Loessner, D. et al. Functionalization, preparation and use of cell-laden gelatin
1344   methacryloyl-based hydrogels as modular tissue culture platforms. *Nature Protocols*. **11** (4),
1345   727–746 (2016).
1346   45.   Yue, K. et al. Synthesis, properties, and biomedical applications of gelatin methacryloyl
1347   (GelMA) hydrogels. *Biomaterials*. **73**, 254–271 (2015).
1348   46.   Sarrigiannidis, S. O. et al. A tough act to follow: collagen hydrogel modifications to
1349   improve mechanical and growth factor loading capabilities. *Materials Today. Bio*. **10**, 100098
1350   (2021).
1351   47.   Karoutas, A. et al. The NSL complex maintains nuclear architecture stability via lamin
1352   A/C acetylation. *Nature Cell Biology*. **21** (10), 1248–1260 (2019).
1353   48.   Ryu, H. et al. Transparent, compliant 3D mesostructures for precise evaluation of
1354   mechanical characteristics of organoids. *Advanced Materials (Deerfield Beach, Fla.)*. **33** (25),
1355   e2100026 (2021).
1356   49.   Carvalho, D. T. O., Feijão, T., Neves, M. I., Da Silva, R. M. P., Barrias, C. C. Directed self-
1357   assembly of spheroids into modular vascular beds for engineering large tissue constructs
1358   Biofabrication Directed self-assembly of spheroids into modular vascular beds for engineering
1359   large tissue constructs. *Biofabrication*. **13** (3), 035008 (2021).

1360   50.   Chaudhuri, O., Cooper-White, J., Janmey, P. A., Mooney, D. J., Shenoy, V. B. Effects of
1361   extracellular matrix viscoelasticity on cellular behaviour. *Nature*. **584** (7822), 535–546 (2020).
1362   51.   Cantini, M., Donnelly, H., Dalby, M. J., Salmeron-Sanchez, M. The plot thickens: The
1363   emerging role of matrix viscosity in cell mechanotransduction. *Advanced Healthcare*
1364   *Materials*. **9** (8), e1901259 (2020).
1365   52.   Elosegui-Artola, A. The extracellular matrix viscoelasticity as a regulator of cell and
1366   tissue dynamics. *Current Opinion in Cell Biology*. **72**, 10–18 (2021).
1367   53.   Chaudhuri, O. Viscoelastic hydrogels for 3D cell culture. *Biomaterials Science*. **5** (8),
1368   1480–1490 (2017).
1369   54.   Nguyen, T. D., Gu, Y. Determination of strain-rate-dependent mechanical behavior of
1370   living and fixed osteocytes and chondrocytes using atomic force microscopy and inverse finite
1371   element analysis. *Journal of Biomechanical Engineering*. **136** (10), 101004 (2014).
1372   55.   Mokbel, M., Hosseini, K., Aland, S., Fischer-Friedrich, E. The Poisson Ratio of the
1373   Cellular Actin Cortex Is Frequency Dependent. *Biophysical Journal*. **118** (8), 1968–1976 (2020).
1374   56.   Javanmardi, Y., Colin-York, H., Szita, N., Fritzsche, M., Moeendarbary, E. Quantifying
1375   cell-generated forces: Poisson's ratio matters. *Communications Physics*. **4**, 237 (2021).
1376

(A)

I)

6 mm

Pour gel solution
and add coverslip

II)

Wait for polymerisation
(20 min)

Coverslip - gel
composite

III)

Solution

Glue

(B)

I)

Seed cells

II)

Serum starve cells
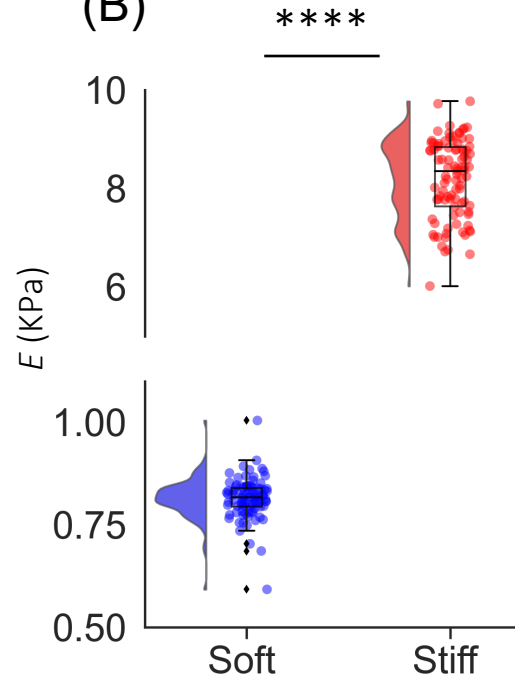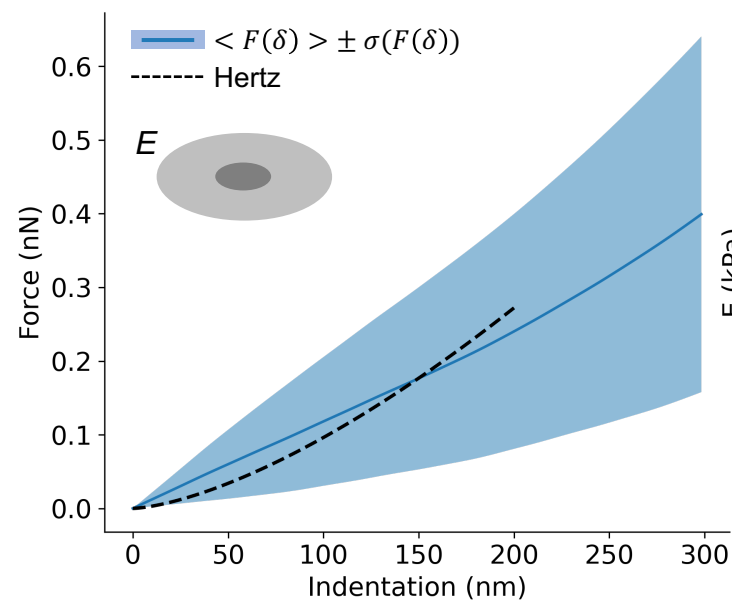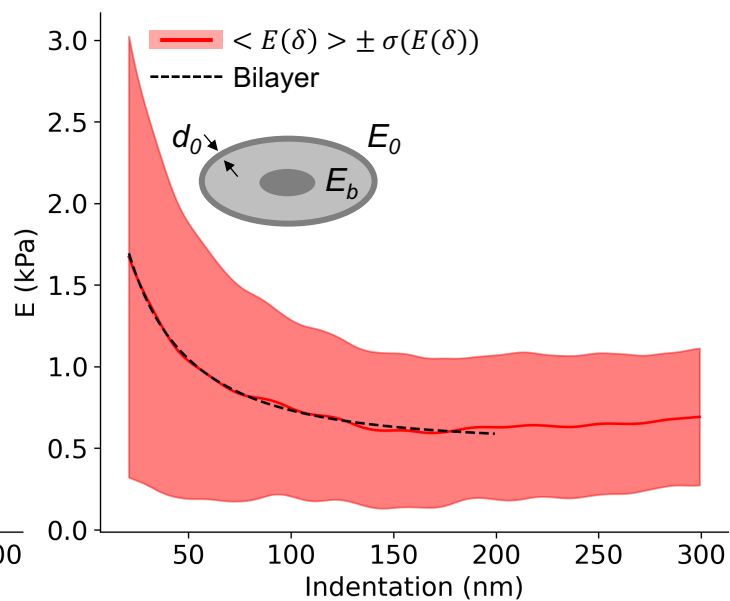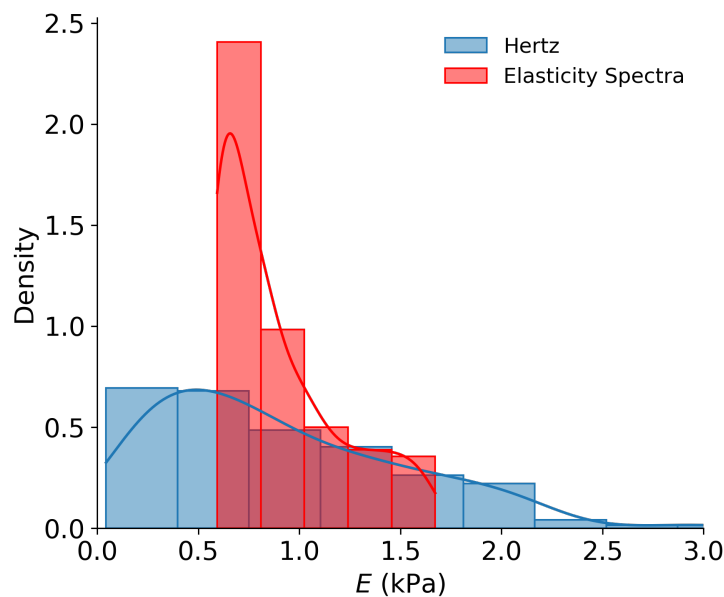(optional)

III)

(A)

(B)

(C)

(A) (B) (C)

(A) (B)
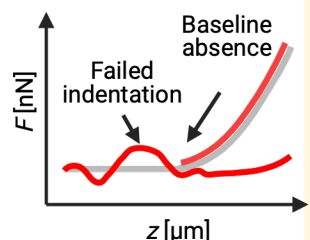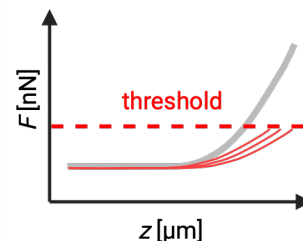
Click here to access/download

Table of Materials

TableofMaterials_RE.xls

Dear JoVE Editors, Dear Dr. Mittal,

We would like to thank the JoVE editorial team for the helpful comments which have improved the quality of the manuscript.

Find below a point-by-point response to each of the editorial comments.

Do not hesitate to contact us if further information is required to make sure the manuscript is ready for publication.

Editorial comments

1. **The manuscript has been formatted according to the journal style. Please retain.**

The revised manuscript's formatting style has been retained to follow the journal style.

2. **Please approve/respond to the specific comments made in the manuscript.**

All comments have been approved/responded to in the revised manuscript.

3. **The maximum page limit for the Protocol section is 10 pages. Please ensure that the Protocol is within this limit.**

The protocol is now within 10 pages. We have moved substantial parts of the protocol to a new file called 'Supplementary protocol.docx'. Additionally, we have made sentences shorter and more concise and moved some notes to the **Discussion** section.

4. **The journal has a hard cut limit of 3 pages for highlighting. Please ensure that the highlighting is up to 3 pages.**

The total lines highlighted should now amount to 3 pages.

5. **Once done, please proofread the manuscript for any grammatical or spelling errors.**

The manuscript has been proofread, and we believe it is free from any grammatical or spelling errors.

TITLE:
Experimental and Data Analysis Workflow for Soft Matter Nanoindentation

AUTHORS AND AFFILIATIONS:
Giuseppe Ciccone[1], Mariana Azevedo Gonzalez Oliva[1], Nelda Antonovaite[2], Ines Lüchtefeld[3], Manuel Salmeron-Sanchez[1], Massimo Vassalli[1]

[1]Centre for the Cellular Microenvironment, James Watt School of Engineering, University of Glasgow, Glasgow, UK
[2]Optics 11 life, De Boelelaan 1081, 1081 HV Amsterdam, The Netherlands
[3]Laboratory of Biosensors and Bioelectronics, ETH Zürich, Gloriastrasse, Zürich, Switzerland

Email addresses of co-authors:
Giuseppe Ciccone   (g.ciccone.1@research.gla.ac.uk)
Mariana Azevedo Gonzalez Oliva   (m.azevedo-gonzalez-oliva.1@research.gla.ac.uk)
Nelda Antonovaite   (nelda@optics11.com)
Ines Lüchtefeld   (luechtefeld@biomed.ee.ethz.ch)
Manuel Salmeron-Sanchez   (manuel.salmeron-sanchez@glasgow.ac.uk)
Massimo Vassalli   (massimo.vassalli@glasgow.ac.uk)

Corresponding authors:
Giuseppe Ciccone   (g.ciccone.1@research.gla.ac.uk)
Mariana Azevedo Gonzalez Oliva   (m.azevedo-gonzalez-oliva.1@research.gla.ac.uk)

SUPPLEMENTARY PROTOCOL:

1.   Preparation of substrates / cells for nanoindentation measurements

1.1.   Preparation of PAAm hydrogels

NOTE: For a detailed protocol on the preparation of elastic PAAm hydrogels of controlled *E*, refer to the work by Tse and Engler[1].

1.1.1.   Preparation of hydrophobic glass slides and acryl-silanized coverslips

1.1.1.1 Submerge the required number of glass slides, for 5 min, in a commercially available hydrophobic-coating solution (see **Table of Materials**). Then, rinse with purified water and let it air dry.

NOTE: The hydrophobic glass slides will be used as the substrate where hydrogels are polymerized.

1.1.1.2. Clean the coverslips of the desired size (12 mm in diameter and 130-160 µm thickness) by sonication, first in purified water and then in absolute ethanol. Wait until the coverslips are fully dry.

CAUTION: Perform steps 1.1.1.3 and 1.1.1.4 in a fume hood, and make sure air flow is

switched on.

1.1.1.3. Place the coverslips in a vacuum pump desiccator. For this protocol, an oil-less piston vacuum pump was used to achieve a maximum vacuum pressure of 60 Torr. Place a glass slide with enough acrylsilane to cover all coverslips (50 µL per 12 mm coverslip).

1.1.1.4 Turn on the vacuum pump and let the reaction take place for a minimum of 3 h.

1.1.1.5 Remove the coverslips from the vacuum chamber and cure them for 1 h at 60°C in an oven.

1.1.2   Preparation of flat PAAm hydrogels

CAUTION: Perform PAAm hydrogels preparation in a fume hood and make sure air flow is switched on.

1.1.2.1 Mix 40% (w/v) acrylamide and 2% (w/v) bis-acrylamide to the appropriate final concentrations[1] in purified water in a reaction tube. The exact volume depends on how many hydrogels are to be tested.

1.1.2.2 For hydrogel polymerization, add 10% (w/v) ammonium persulfate (APS) (1:100 total volume) and tetramethylethylenediamine (TEMED) (1:1000 total volume) to the acrylamide mixture.

1.1.2.3 Vortex for 5 s and quickly move on to the next step to prevent polymerization of the gel in the reaction tube.

1.1.2.4 Pipette the desired volume onto a hydrophobic glass slide. Pipette 20 µL of the hydrogel solution to create a ~200 µm thick hydrogel (**Figure 2A**, left).

1.1.2.5 To flatten the hydrogel, place the silane treated coverslip on top of the pipetted drop of the hydrogel and wait ~ 20 min for polymerization to take place (**Figure 2A**, left).

1.1.2.6 Gently peel the coverslip off the hydrophobic glass slide to find a coverslip-gel composite (**Figure 2A**, center).

1.1.2.7 Place the coverslip-gel composite in purified water overnight for the hydrogels to swell. The hydrogels can be stored at 4 °C until mechanical characterization.

NOTE: 5–6 hydrogels can by polymerized on the same glass slide.

1.1.3   PAAm sample preparation for mechanical characterization

1.1.3.1 For mechanical characterization, the material must be stably attached to a surface. To achieve this, attach the coverslip-gel composite to a Petri dish by using super glue or thin double-sided tape. Handle the coverslip-gel composite with tweezers and submerge it in purified water before testing to avoid drying (**Figure 2A**, right).

1.2   Preparation of cells

NOTE: To perform single cell indentation measurements, culture cells in the appropriate media in treated tissue culture dishes. For Human Embryonic Kidney (HEK 293T) cells, follow the steps outlined below.

1.2.1   Thaw and split cells to culture them at a density of 6,000 cells/cm^2 in a cell culture treated 35 mm dish. Keep cells in a high glucose DMEM containing sodium pyruvate, L-glutamine, 10% fetal bovine serum (FBS) and 1% penicillin/streptomycin (P/S).

1.2.2   Leave cells to adhere for a minimum of 4 h to perform nanoindentation measurements. Culture cells until reaching 70% confluence for performing single cell measurements, as it may become challenging to indent single cells once a confluent monolayer starts to form (**Figure 2B**).

NOTE: Cell cycle might influence the mechanical properties of cells[2]. To reduce variability within the same cell population, cells can be serum starved in 1% FBS media overnight, to achieve cell cycle synchronization prior to performing measurements[3].

2. Starting up the device, probe choice and probe calibration

2.1 Starting the system

2.1.1   Switch on the nanoindentation device and associated optical microscope.

2.1.2   Switch on the computer associated with the device.

2.1.3   Switch on the interferometer.

2.1.4   Switch on the controller box.

2.1.5   Switch on the inverted optical microscope associated with the nanoindenter. The specific instructions depend on the microscope's manufacturer, and the imaging modality used.

2.1.6   If applicable, switch on the air compressor of the anti-vibration table on which the microscope and nanoindentation device are mounted on. Wait for the compressor's pressure indicator to reach the desired level. Check that the anti-vibration table is working by gently tapping on it. The table should quickly stabilize back to its original position.

2.1.7   Open the nanoindentation software (version 3.4.1 is used in this protocol) on the computer by double clicking on the associated desktop icon. Wait for all hardware to be ready, which means they will show as **Idle** in the status bar of the pop-up window on the screen.

2.1.8   A second pop-up window will appear asking to home the stage. Answering **Yes** will

move the nanoindentation stage to the front left corner setting both *x* and *y* coordinates to 0, and move to the last *(x,y)* point in the matrix scan parameters. Answering **No** will not move the arm. Click on **Yes**, taking care that the arm will not bump into anything while automatically moving to the front left corner.

2.2 Go back to the main **Protocol** for steps on how to select the appropriate nanoindentation probe.

2.3   Mount the nanoindentation probe as follows.

2.3.1   Carefully remove the chosen probe from the housing box by holding the plastic probe holder with one hand and the connector with the other hand. Take extra care when handling the probe as accidental contact with the cantilever or bending of the fiber wire will most likely break it.

2.3.2   Insert the plastic probe holder in the dedicated housing on the nanoindenter's arm. Make sure the probe is mounted in the correct way, with the spherical tip pointing downwards. Carefully connect the green optical fiber connector in the appropriate socket. Take extra care not to pull or bend the optical fiber.

2.3.3   Bring the probe in the center of the microscope's field of view by gently moving the nanoindenter's arm by hand or using the digital *x/y* control arrows in software's main window. Do not focus the *z* position of the probe at this point, as this will change both during the calibration procedure and the actual experiment.

2.4   Go back to the main **Protocol** for steps on how to calibrate the probe.

3.   Measuring the Young's Modulus of soft materials

3.1 Cleaning the probe and switching off the instrument

3.1.1   After completing all measurements, discard or store the sample away.

3.1.2   Clean the probe with isopropanol followed by water using a Pasteur pipette.

3.1.3   Once the probe has been cleaned, make sure the probe is free of any remaining residue with the aid of the microscope before carefully storing it away in the same position it was shipped in (the box should provide the appropriate grooves to prevent the probe from breaking whilst stored). The probe will dry while securely stored.

3.1.4   If the probe has some remaining sample residue, carefully clean it with a tissue making sure it only touches the debris and not the probe or repeat the cleaning step. If the cantilever is bent, return it to its original position with the aid of a tissue. If the probe is wet, the cantilever may be more prone to bending, especially when it is soft. In this case, wait for the probe to dry and for the cantilever to return to its horizontal position on its own rather than trying to unbend it while wet, as this can lead to probe damage.

3.1.5   Once the probe is stored away, turn off the equipment in the reverse order compared to when switched on: i.e., software, microscope, controller, interferometer, and optical microscope.

4.   Data analysis

4.1 Downloading and installing the software

NOTE: The data analysis of *F-z* data is performed through an open-source software programmed in Python and equipped with a user-friendly GUI. The software consists of two GUIs, one advised to be installed on the lab computer (data preparation) and one advised to be installed on the computer where the formal data analysis will be performed (data analysis).

4.1.1   The software is programmed in Python, and the interpreter for this language must be installed on computers where the software is intended to be used. Navigate to www.python.org and install the latest stable release of Python 3 for your operating system. Older versions of Python 2 are not supported.

NOTE: Further instructions on how to install Python can be found on www.python.org.

4.1.2   Install GitHub Desktop from https://desktop.github.com. This will be used to easily keep the software up to date without having to re-download new versions. Create an account at https://github.com following the instructions after clicking on **Sign Up**.

4.1.3   Create two empty folders on your local computer/s, named NanoPrepare and NanoAnalysis. The names are arbitrary, although stick to something simple.

4.2   Open GitHub Desktop on your computer and login with your account. This allows to clone the repositories associated with the nanoindentation software on your computer, and to use the software locally. Click on **Add, Clone Repository…, URL**. In the **URL or username/repository** enter: https://github.com/CellMechLab/NanoPrepare[4].

4.3   In the **Local Path** enter the directory of NanoPrepare. Once the cloning is completed, repeat this step and clone the following repository: https://github.com/CellMechLab/nanoindentation[5] adding it to the local directory NanoAnalysis.

NOTE: Installing the software through GitHub Desktop is optional, but recommended as it easily allows to keep the software up to date. Alternatively, after installing Python 3, the software can be directly downloaded from the GitHub links given in step 4.1.2 above and launched following the instructions given in steps 2.1 and 3.1 (see later).

4.4   Both software require a number of dependencies in order to run, including: SciPy[6], NumPy[7], PyQt5[8] and PyQtGraph[9]. The easiest way to install those dependencies is to use the PIP utility, which can be called from the command line. For example, to install SciPy[6], run the command: **pip install scipy** (windows) or **pip3 install scipy** (MacOS). Further information on how to install packages can be found at: https://packaging.python.org/tutorials/installing-

[packages/](). Install the latest stable versions for all packages.

Supplementary references

1. Tse, J.R., Engler, A.J. Preparation of hydrogel substrates with tunable mechanical properties. *Current Protocols in Cell Biology*. (SUPPL. 47), 1–16 (2010).
2. Clark, A.G., Paluch, E. Mechanics and Regulation of Cell Shape During the Cell Cycle. *Cell Cycle in Development, Results and Problems in Cell Differentiation*. **53**, 31–73 (2011).
3. Langan, T.J., Chou, R.C. Synchronization of Mammalian Cell Cultures by Serum Deprivation. *Cell Cycle Synchronization*. **761**, 75–83 (2011).
4. Vassalli, M., Ciccone, G. CellMechLab/NanoPrepare: v0.1.1. ZENODO.5546497 (2021).
5. Vassalli, M., Ciccone, G., Lüchtefeld, I. CellMechLab/nanoindentation: v1.0.0. ZENODO.5546496 (2021).
6. Virtanen, P. et al. SciPy 1.0: fundamental algorithms for scientific computing in Python. *Nature Methods*. **17** (3), 261–272 (2020).
7. Harris, C.R. et al. Array programming with NumPy. *Nature*. **585** (7825), 357–362 (2020).
8. Riverbank Computing PyQt5. at <https://pypi.org/project/PyQt5/> (2021).
9. PyQtGraph. at <https://www.pyqtgraph.org/>.

Supplementary Note 1: Adding custom filters and CP algorithms to NanoAnalysis

Custom CP algorithms and filters can be easily added to the GUI. CP finding routines and filters are in separate modules called panels.py (CP algorithms) and filter_panel.py (filters), respectively.

1. Adding a new CP algorithm

1.1   Using an editor of choice, such as Visual Studio Code (https://code.visualstudio.com/) open panels.py.

1.2   Scroll down to the end of the module where a template for a new algorithm is given. The rationale behind the template is explained with an example in the following steps.

1.3   Create a new Class that inherits the ContactPoint class. The Class will contain the new CP finding algorithm. For example, for the RoV algorithm, a new class is created called ThRoV which inherits the ContactPoint class:

```
1.   class ThRoV(ContactPoint):
2.       """Ratio of Variances (RoV) algorithm. doi: https://doi.org/10.1038/srep21267."""
```

1.4   Add the parameters that will be used in the CP algorithm. Those can be Floats, Integers or Combo (both). For example, the RoV algorithm is based on a 'Safe Threshold' parameter, a 'X Range' parameter and a 'Window RoV' parameter, as explained in the main text. To do so, use the create method. After adding the parameters, the code looks like:

```
1.   class ThRov(ContactPoint):
2.       """Ratio of Variances (RoV) algorithm. doi: https://doi.org/10.1038/srep21267."""
3.       def create(self):
4.           self.Fthreshold = CPPFloat('Safe Threshold [nN]')
5.           self.Fthreshold.setValue(10.0)
6.           self.Xrange = CPPFloat('X Range [nm]')
7.           self.Xrange.setValue(1000.0)
8.           self.windowr = CPPInt('Window RoV [nm]')
9.           self.windowr.setValue(200)
10.          self.addParameter(self.Fthreshold)
11.          self.addParameter(self.Xrange)
12.          self.addParameter(self.windowr)
```

To understand the above lines of code, consider the 'Safe Threshold' parameter as an example. Line 4 self.Fthreshold = CPPFloat('Safe Threshold [nN]') does the following: creates the variable Fthreshold (as per referenced in the code), which is a float (CPPFloat) that will be displayed in the GUI as 'Safe Threshold [nN]'. Line 5 sets its default value to 10.0 nN. To add the parameter to the GUI, the addParameter() method is used (line 10). The same rationale applies to the other parameters.

1.5   In principle, after setting the required parameters (step 4), the CP algorithm per se can be written in the calculate method, which takes the curve object (c) and returns a list with the x and y coordinates of the CP. In practice, intermediate steps are often required, such as selecting a ROI where to look for the CP and calculating the weight on which the algorithm is based (in this case, the ratio of variances). To select the ROI, we often use the same block of code in the getRange method:

```
1.   class ThRov(ContactPoint):
2.       """Ratio of Variances (RoV) algorithm. doi: https://doi.org/10.1038/srep21267."""
3.       def create(self):
4.           self.Fthreshold = CPPFloat('Safe Threshold [nN]')
5.           self.Fthreshold.setValue(10.0)
6.           self.Xrange = CPPFloat('X Range [nm]')
7.           self.Xrange.setValue(1000.0)
8.           self.windowr = CPPInt('Window RoV [nm]')
9.           self.windowr.setValue(200)
10.          self.addParameter(self.Fthreshold)
11.          self.addParameter(self.Xrange)
12.          self.addParameter(self.windowr)
13.
14.      def getRange(self, c):
15.          x = c._z
16.          y = c._f
17.          try:
18.              jmax = np.argmin((y - self.Fthreshold.getValue()) ** 2)
19.              jmin = np.argmin((x - (x[jmax] - self.Xrange.getValue())) ** 2)
20.          except ValueError:
21.              return False
22.          return jmin, jmax
```

Lines 14-22 define the ROI where the CP will be searched for. Specifically, lines 15 and 16 extract the displacement (`c._z`) and force (`c._f`) from the curve (c) object. Line 18 takes the index of the point closest to the 'Safe Threshold [nN]' (`jmax`), and line 19 takes the index of the point which is closest to the displacement z corresponding to the safe threshold, shifted left by a value defined by 'X Range [nm]' (`jmin`). Thus, `jmin` and `jmax` define the ROI where the CP will be searched for, and should be returned from `getRange`.

1.6   Calculate and store the weight in the ROI. This is done with the `getWeight` method. For example, in the case of the RoV algorithm, one wants to calculate the ratio between the variances of the force signal to the right and to the left of the trial CP in a given window ('Window RoV'), for all trial points in the ROI. Therefore, the code looks like:

```
1.   class ThRov(ContactPoint):
2.       """Ratio of Variances (RoV) algorithm. doi: https://doi.org/10.1038/srep21267."""
3.       def create(self):
4.           self.Fthreshold = CPPFloat('Safe Threshold [nN]')
5.           self.Fthreshold.setValue(10.0)
6.           self.Xrange = CPPFloat('X Range [nm]')
7.           self.Xrange.setValue(1000.0)
8.           self.windowr = CPPInt('Window RoV [nm]')
9.           self.windowr.setValue(200)
10.          self.addParameter(self.Fthreshold)
11.          self.addParameter(self.Xrange)
12.          self.addParameter(self.windowr)
13.
14.      def getRange(self, c):
15.          x = c._z
16.          y = c._f
17.          try:
18.              jmax = np.argmin((y - self.Fthreshold.getValue()) ** 2)
19.              jmin = np.argmin((x - (x[jmax] - self.Xrange.getValue())) ** 2)
20.          except ValueError:
21.              return False
22.          return jmin, jmax
23.
24.      def getWeight(self, c):
25.          jmin, jmax = self.getRange(c)
26.          winr = self.windowr.getValue()
27.          x = c._z
28.          y = c._f
```

```
29.          if (winr + jmax) > len(y):  # check1
30.              return False
31.          if jmin < winr:  # check2
32.              return False
33.          rov = []
34.          for j in range(jmin, jmax):
35.              rov.append((np.var(y[j+1: j+winr])) / (np.var(y[j-winr: j-1])))
36.          return x[jmin:jmax], rov
```

1.7 Finally, the point where the weight is optimised (i.e., where it is either maximum or minimum depending on the algorithm) corresponds to the CP. It is required to return a list containing the *x* and *y* coordinates of the CP, which can be done with the `calculate` method. For example, the complete RoV algorithm looks like:

```
1.  class ThRov(ContactPoint):
2.      """Ratio of Variances (RoV) algorithm. doi: https://doi.org/10.1038/srep21267."""
3.      def create(self):
4.          self.Fthreshold = CPPFloat('Safe Threshold [nN]')
5.          self.Fthreshold.setValue(10.0)
6.          self.Xrange = CPPFloat('X Range [nm]')
7.          self.Xrange.setValue(1000.0)
8.          self.windowr = CPPInt('Window RoV [nm]')
9.          self.windowr.setValue(200)
10.         self.addParameter(self.Fthreshold)
11.         self.addParameter(self.Xrange)
12.         self.addParameter(self.windowr)
13.
14.     def getRange(self, c):
15.         x = c._z
16.         y = c._f
17.         try:
18.             jmax = np.argmin((y - self.Fthreshold.getValue()) ** 2)
19.             jmin = np.argmin((x - (x[jmax] - self.Xrange.getValue())) ** 2)
20.         except ValueError:
21.             return False
22.         return jmin, jmax
23.
24.     def getWeight(self, c):
25.         jmin, jmax = self.getRange(c)
26.         winr = self.windowr.getValue()
27.         x = c._z
28.         y = c._f
29.         if (winr + jmax) > len(y):  # check1
30.             return False
31.         if jmin < winr:  # check2
32.             return False
33.         rov = []
34.         for j in range(jmin, jmax):
35.             rov.append((np.var(y[j+1: j+winr])) / (np.var(y[j-winr: j-1])))
36.         return x[jmin:jmax], rov
37.
38.     def calculate(self, c):
39.         z = c._z
40.         f = c._f
41.         try:
42.             zz_x, rov = self.getWeight(c)
43.         except TypeError:
44.             return
45.         rov_best_ind = np.argmax(rov)
46.         j_rov = np.argmin((z-zz_x[rov_best_ind])**2)
47.         return [z[j_rov], f[j_rov]]
```

1.8 For the algorithm to be added to the GUI, it must be appended to the ALL list as a dictionary containing the name to be displayed on the GUI and the Class corresponding to the

given algorithm. For example, for the RoV algorithm, the following line of code should be added to the end of the module:

```
1.  ALL.append({'label': 'Ratio of Variances', 'method': ThRov})
```

The algorithm can now be used as part of the GUI.

NOTE: Return `False` when the algorithm fails to complete a step (e.g., line 20). This will ensure that curves where the algorithm fails will be moved to the 'Included' set, as explained in the main protocol.

2.   Adding a new Filter

The procedure of adding a custom filter to the GUI is akin to that of adding a new CP algorithm.

2.1   Using an editor of choice, such as Visual Studio Code (https://code.visualstudio.com/) open filter_panel.py.
2.2   Scroll down to the end of the module where a template for a new algorithm is given. The rationale behind the template is explained with an example in the following steps.
2.3   Create a new Class that inherits the Filter class. The Class will contain the new filter algorithm. For example, for the savgol filter (see main text) the code looks like:

```
1.  class SavGolFilter(Filter):
2.      """
3.      Filters data with the Savitzky-Golay filter from the Scipy Library.
4.      doi: https://doi.org/10.1038/s41592-019-0686-2
5.      """
```

2.4   Add the filter parameters that the user can change in the GUI. For the savgol filter, those are the polynomial order and the window length. The code looks like:

```
1.  class SavGolFilter(Filter):
2.      """
3.      Filters data with the Savitzky-Golay filter from the Scipy Library.
4.      doi: https://doi.org/10.1038/s41592-019-0686-2
5.      """
6.      def create(self):
7.          self.win = FilterInt('Window Length [nm]')
8.          self.win.setValue(25)
9.          self.polyorder = FilterInt('Polynomical Order (Int)')
10.         self.polyorder.setValue(3)
11.         self.addParameter(self.win)
12.         self.addParameter(self.polyorder)
```

2.5   Finally, calculate the filtered data with the `calculate` method, which returns the filtered force data:

```
1.  class SavGolFilter(Filter):
2.      """
3.      Filters data with the Savitzky-Golay filter from the Scipy Library.
4.      doi: https://doi.org/10.1038/s41592-019-0686-2
5.      """
6.      def create(self):
7.          self.win = FilterInt('Window Length [nm]')
```

```
8.         self.win.setValue(25)
9.         self.polyorder = FilterInt('Polynomical Order (Int)')
10.        self.polyorder.setValue(3)
11.        self.addParameter(self.win)
12.        self.addParameter(self.polyorder)
13.
14.    def calculate(self, c):
15.        y = c._f
16.        win = self.win.getValue()
17.        polyorder = self.polyorder.getValue()
18.        if win % 2 == 0:
19.            win += 1
20.        if polyorder > win:
21.            return False
22.        y_smooth = savgol_filter(y, win, polyorder)
23.        return y_smooth
```

2.6   If additional methods are needed to filter the data, those can be added within the algorithm. For the new filter to be added to the GUI it must be appended to the ALL_FILTERS list as a dictionary containing the name to be displayed on the GUI and the Class corresponding to the given algorithm. For example, for the savgol algorithm, the following line of code should be added to the end of the module:
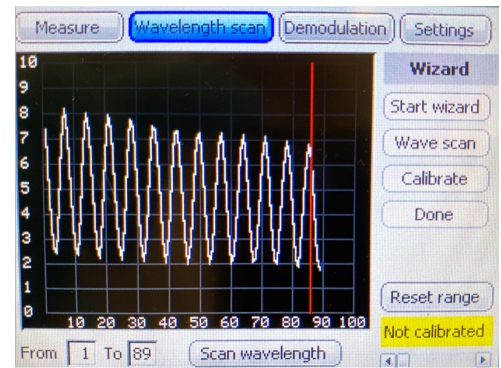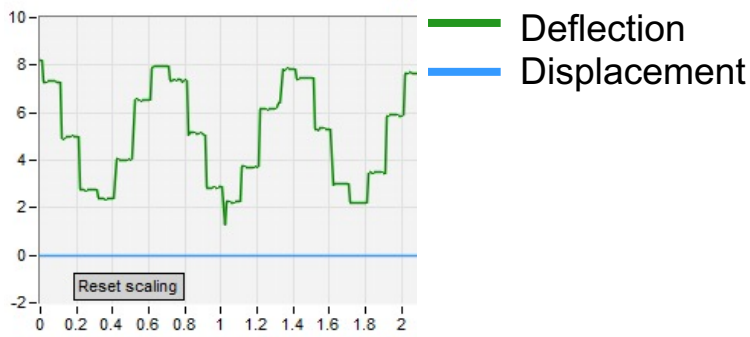
```
1.   ALL_FILTERS.append({'label': 'Savitzky Golay', 'method': SavGolFilter})
```
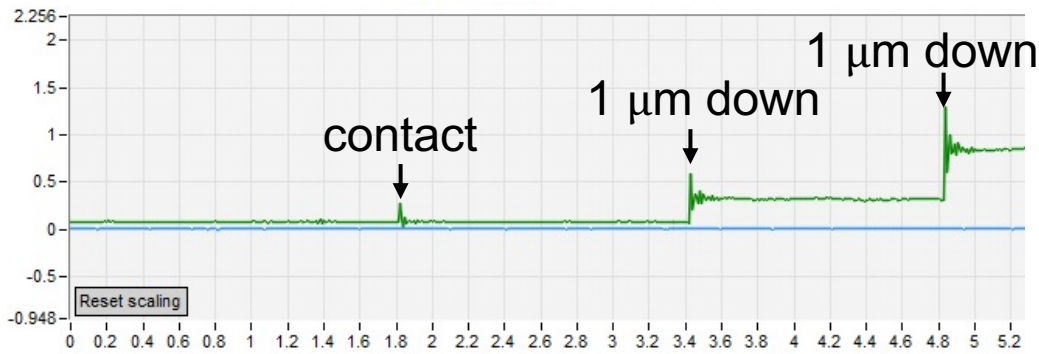
NOTE: Return False in case of any exceptions. For example, the savgol filter from the SciPy library required the polynomial order to be less than the window length. Lines 20-21 handle this.
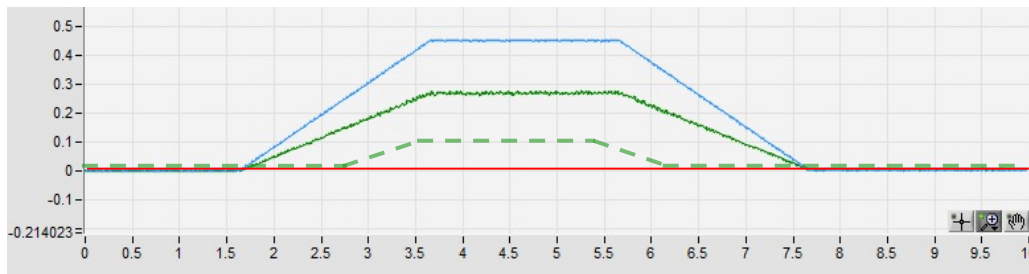
(A) Wavelength scan

(B) Find surface

(C) Geometrical calibration

(D) Demodulation